

# Thermodynamics of deformed $\text{AdS}_5$ model with a positive/negative quadratic correction in graviton-dilaton system

---

Danning Li <sup>1</sup>, Song He <sup>1,2</sup>, Mei Huang<sup>1,3</sup>, Qi-Shu Yan <sup>2</sup>

<sup>1</sup> *Institute of High Energy Physics, Chinese Academy of Sciences, Beijing, China*

<sup>2</sup> *College of Physical Sciences, Graduate University of Chinese Academy of Sciences, Beijing, China*

<sup>3</sup> *Theoretical Physics Center for Science Facilities, Chinese Academy of Sciences, Beijing, China*

**ABSTRACT:** By solving the Einstein equations of the graviton coupling with a real scalar dilaton field, we establish a general framework to self-consistently solve the geometric background with black-hole for any given phenomenological holographic models. In this framework, we solve the black-hole background, the corresponding dilaton field and the dilaton potential for the deformed  $\text{AdS}_5$  model with a positive/negative quadratic correction. We systematically investigate the thermodynamical properties of the deformed  $\text{AdS}_5$  model with a positive and negative quadratic correction, respectively, and compare with lattice QCD on the results of the equation of state, the heavy quark potential, the Polyakov loop and the spatial Wilson loop. We find that the bulk thermodynamical properties are not sensitive to the sign of the quadratic correction, and the results of both deformed holographic QCD models agree well with lattice QCD result for pure  $\text{SU}(3)$  gauge theory. However, the results from loop operators favor a positive quadratic correction, which agree well with lattice QCD result. Especially, the result from the Polyakov loop excludes the model with a negative quadratic correction in the warp factor of  $\text{AdS}_5$ .

**KEYWORDS:** Graviton-dilaton system, black-hole, equation of state.

---

## Contents

<b>1. Introduction</b>	<b>2</b>
<b>2. 5D Einstein dilaton system with black-hole background</b>	<b>4</b>
2.1 Minimal non-critical string framework	4
2.2 Graviton-dilaton system with dual black-hole for hQCD model	6
<b>3. Dual black-hole solution for the hQCD model with quadratic correction</b>	<b>8</b>
<b>4. Equation of state for hQCD model with quadratic correction</b>	<b>10</b>
4.1 The would-be critical temperature	11
4.2 The entropy density	15
4.3 The pressure density, energy density and trace anomaly	16
4.4 The sound velocity and specific heat	17
4.5 Discussion	19
<b>5. Heavy quark potential, Polyakov loop, spatial string tension at finite temperature</b>	<b>20</b>
5.1 The heavy quark potential	21
5.2 The Polyakov loop	23
5.3 The spatial Wilson loop	26
<b>6. Conclusion and discussion</b>	<b>28</b>
<b>Appendices</b>	<b>30</b>
<b>A. Some simple analytical black hole solutions</b>	<b>31</b>
<b>B. Free energy density at UV boundary for the hQCD model with <math>A_s(z) = ck^2z^2</math></b>	<b>32</b>
<b>C. To extract the spatial string tension</b>	<b>33</b>

# 1. Introduction

In recent decade, the discovery of the anti-de Sitter/conformal field theory (AdS/CFT) correspondence and the conjecture of the gravity/gauge duality [1] has been widely used to understand strongly coupled dense and hot quark matter [2, 3, 4, 5, 6, 7, 8, 9, 10, 11, 12, 13, 14].

One of the most successful examples of using thermal  $\mathcal{N} = 4$  super-Yang-Mills theory (SYM) in quantum chromodynamics (QCD) at finite temperature is the small value of shear viscosity over entropy density  $\eta/s = 1/4\pi$  [2], which is very close to the value used to fit the RHIC data of elliptic flow  $v_2$  [15, 16]. It is now believed that the system created at RHIC is a strongly coupled quark-gluon plasma (sQGP) and behaves like a nearly "perfect" fluid [17, 18]. However, lattice QCD results show that the bulk viscosity over entropy density ratio  $\zeta/s$  rises dramatically up to the order of 1.0 near the critical temperature  $T_c$  [19, 20, 21]. The sharp peak of bulk viscosity at  $T_c$  has also been observed in QCD effective models [22, 23, 24]. The large bulk viscosity near phase transition is related to the non-conformal equation of state [25, 26], e.g, the square of sound velocity is around 0.07, which is much smaller than the conformal value 1/3. In the SYM plasma, the square of sound velocity is always 1/3 and the bulk viscosity  $\zeta$  always vanishes at all temperatures.

These facts demonstrate that strongly coupled quark gluon plasma near  $T_c$  is not conformal invariant. In order to mimic the QCD equation of state, much effort has been put to find the gravity dual of gauge theories which break the conformal symmetry, e.g, [5, 6, 7, 8], where a real scalar dilaton field background has been introduced to couple with the graviton. Refs.[5] and [6, 7] have used different dilaton potentials as input, while Ref.[8] has used QCD  $\beta$ -function as input.

The AdS/CFT approach has also been widely applied to describe non-perturbative phenomenology in the vacuum, where conformal symmetry is also needed to be broken [27, 28, 29, 30, 31, 32, 33, 34, 35, 36, 37, 38, 39, 40, 41, 42, 43, 44]. The most economic way of breaking the conformal symmetry is to add a proper deformed warp factor in front of the AdS<sub>5</sub> metric structure, which can capture the main features of non-perturbative QCD physics. For example, Andreev-Zakharov proposed a positive quadratic correction,  $e^{cz^2}$  with  $z$  the fifth dimension coordinate and  $c > 0$ , in the deformed warp factor of AdS<sub>5</sub> geometry, which can help to realize the linear heavy quark potential [35]. The linear heavy quark potential can also be obtained by introducing other deformed warp factors, e.g. the deformed warp factor which mimics the QCD running coupling [43], and the logarithmic correction with an explicit IR cutoff  $\log \frac{z_{IR}-z}{z_{IR}}$  [44]. To produce the linear Regge behavior of the hadron excitations, Karch-Katz-Son-Stephanov [34] proposed the soft-wall AdS<sub>5</sub> model or KKSS model by introducing a quadratic dilaton background in the 5D meson action, whose effect in some sense looks like introducing a negative quadratic correction,  $e^{-cz^2}$ , in the warp factor of the AdS<sub>5</sub> geometry. However, it is worthy of mentioning that the

model with a quadratic correction in the warp factor of the metric is not equivalent to the model with a quadratic correction in the dilaton background. A positive quadratic correction  $e^{cz^2}$  in the dilaton background of the 5D hadron action has also been used to investigate hadron spectra [36, 37], however, higher spin excitations in this background will get imaginary mass [33, 45].

From the above studies of constructing the holographic QCD (hQCD) models for describing the heavy quark potential and the light hadron spectra, we have observed that a quadratic background correction is related to the confinement property, i.e. the linear quark anti-quark potential and the linear Regge behavior. Furthermore, we have observed that to produce the linear heavy quark potential, the positive quadratic correction has been introduced in the deformed warp factor, while to produce the linear Regge behavior, the negative quadratic correction is introduced in the dilaton background in the 5D hadron action.

It is natural to ask the connection between the quadratic correction in the metric and dilaton background, and which sign is consistent with real QCD data. If we assume that there is no direct connection between the dilaton field and metric background, these two types of models cannot be contrasted. However, the metric structure of the hQCD model and its corresponding dilaton background can be self-consistently solved from the Einstein equation in the non-critical string framework or the 5D Einstein dilaton system, e.g, as described in Ref. [41]. In this framework, the connection between the metric structure and the dilaton background can be established.

In Ref.[44], we have numerically solved the dilaton background at zero temperature for the deformed  $AdS_5$  model with positive and negative quadratic correction, respectively. In this paper, we extend our previous study in the non-critical string framework at zero temperature to finite temperature, and self-consistently solve the black-hole background, dilaton field and the dilaton potential. In order to further pin down the sign of the quadratic correction in the hQCD model, we systematically investigate the thermodynamic properties of these two deformed  $AdS_5$  models, including the equation of state, the heavy quark potential, the spatial string tension, and the Polyakov loop at finite temperature. By comparing with lattice results, we find that the equation of state is not sensitive to the sign of the quadratic correction. However, the results from loop operators favor a positive quadratic correction. Especially, the result from the Polyakov loop excludes the model with negative quadratic correction in the warp factor of  $AdS_5$ .

The paper is organized as follows. In Sec.2, we derive the general formulae for equations of motion in classical 5D gravity-dilaton system, and solve the black-hole background, the dilaton field and its corresponding dilaton potential for any given hQCD model. In Sec.3, we self-consistently solve the dual black-hole background, the dilaton field and its dilaton potential for the hQCD models with positive and negative quadratic correction in the deformed warp factor of  $AdS_5$  metric background. In

Sec.4, we study the phase transition and the equation of state, including the entropy density, the pressure density, the energy density and the square of sound velocity for the two hQCD models with quadratic corrections. In Sec.5, we calculate the heavy quark potential, the Polyakov loop and the spatial Wilson loop at finite temperature and compare our results with lattice data. The summary and discussion is given in Sec.6. We also list several special exact solutions of the general graviton-dilaton system in Appendix A, and the method of extracting the spatial string tension in Appendix C.

## 2. 5D Einstein dilaton system with black-hole background

### 2.1 Minimal non-critical string framework

For low energy IIA/IIB supergravity, the classical action in the string frame has the following form [46]:

$$S_{IIA/IIB} = S_{NS} + S_R + S_{CS} + S_{fermion}. \quad (2.1)$$

Where  $S_{fermion}$  is the action from the fermionic part, and  $S_{NS}, S_R, S_{CS}$  are bosonic part actions for Neveu-Schwarz (NS) sector of graviton-dilaton coupling, Ramond (R) kinetic term for the form field, Chern-Simons term, respectively. The NSNS sector action takes the form of

$$S_{NS} = \frac{1}{2k_{10}^2} \int d^{10} \sqrt{-G_s} e^{-2\phi} \left( R + 4\partial_\mu \phi \partial^\mu \phi - \frac{1}{2} |H_3|^2 \right). \quad (2.2)$$

The RR part action and Chern-Simons term take different forms for Type-IIA and IIB supergravity, respectively:

$$\begin{aligned} S_R|_{IIA} &= \frac{1}{2k_{10}^2} \int d^{10} \sqrt{-G_s} \left( |F_2|^2 + |\widetilde{F}_4|^2 \right), \\ S_{CS}|_{IIA} &= \frac{1}{2k_{10}^2} \int B_2 \wedge F_4 \wedge F_4, \\ S_R|_{IIB} &= \frac{1}{2k_{10}^2} \int d^{10} \sqrt{-G_s} \left( |F_1|^2 + \frac{1}{2} |\widetilde{F}_3|^2 + |\widetilde{F}_5|^2 \right), \\ S_{CS}|_{IIB} &= \frac{1}{2k_{10}^2} \int C_4 \wedge H_3 \wedge F_3. \end{aligned} \quad (2.3)$$

Where  $k_{10}$  the 10-dimension Newton coupling constant,  $G_s$  the metric in the string frame,  $R, \phi$  are scalar curvature and the dilaton field, respectively.  $B$  is anti-symmetric 2-form tensor field,  $C$  is R-R form field,  $H, F$  are field strengths of  $B, C$ , and  $F = e^{-\phi} \widetilde{F}$ .  $F_2, F_4$  only appear in IIA and  $F_1, F_3, F_5$  only appear in IIB supergravity.

We are interested in building a 5-dimensional effective gravity dual to a 4-dimensional non-Abelian gauge theory. We follow the argument in Ref.[41] to derive the minimal 5D effective graviton-dilaton system from 10D supergravity Eq.(2.1).

1) For pure Yang-Mills gauge theory, there is no fermionic degrees of freedom, therefore, we neglect the  $S_{fermion}$  in Eq.(2.1) for simplicity.

2) In the NSNS sector, one should note that we ignore the effect of  $H_3 = dB_2$ , which is normally taken to be zero because it induces noncommutative effect in the string theory. This leads to the vanishing of the Chern-Simons action, i.e.  $S_{CS} = 0$ .

3) The RR part includes six fields strengths  $F_0, F_1, F_2, F_3, F_4, F_5$ , where only  $F_0, F_1, F_2$  are independent due to the Poincare dual relationship.  $F_0$  couples to bulk instantons, and its dual  $F_5$   $F_0$  generates a four-form field stems from  $D_3$  branes related to the  $U(N_c)$  gauge group.  $F_1 = dC_0$  originates from axion field  $C_0 = a$  which is dual to  $Tr[F \wedge F]$  in the gauge theory.  $F_4 \sim F_1$  and its associated three-form  $C_3$  couples to domain walls.  $F_2$  generates a vector and couples minimally to the baryon density, and it breaks Lorentz invariance in the QCD vacuum. Therefore,  $F_2$  and its dual  $F_3$  can be safely neglected.

From the above analysis, the relevant low-lying fields, which are expected to be dual to the lowest dimension operators in the gauge theory, are the graviton  $g_{\mu\nu}$ , the dilaton  $\phi$ , and the RR axion  $a$ . One can put the solution of  $F_5$  into Eq.(2.1) and then integrate out the inner five compact space-time  $M_5$ . Finally, one can obtain the minimal non-critical 5D effective gravity action as following:

$$S_{5D} = \frac{1}{16\pi G_5} \int d^5x \sqrt{-g^S} e^{-2\phi} (R + 4\partial_\mu \phi \partial^\mu \phi - V_S(\phi)) \quad (2.4)$$

Where  $G_5$  is 5D Newton constant,  $g^S$  and  $V_S(\phi)$  are the 5D metric and dilaton potential in the string frame, respectively.

In the minimal non-critical string framework, the metric structure, the dilaton field and the dilaton potential should be solved self-consistently from the Einstein equations. One can use the dilaton potential as input to solve the metric structure and the dilaton field. There are several different choices for the dilaton potential from several groups. The scalar field or dilaton field  $\phi$  encodes the running of the Yang-Mills gauge theory's coupling  $\lambda$ . In the framework of Gürsoy -Kiritsis-Nitti (GKN) [41, 6, 7], the renormalized dilaton field  $\phi$  has been defined as  $\lambda = e^\phi$ , and the dilaton potential can be solved from the input of QCD running coupling function, i.e.  $\beta(\lambda)$ -function. In Ref. [5], in order to mimic the QCD equation of state, the authors chooses the dilaton potential as  $V(\phi) = \frac{-12\cosh\gamma\phi + b\phi^2}{L^2}$  where  $L$  is the radius of the  $AdS_5$ .

However, in the graviton-dilaton coupling system, for the given dilaton potential in [5, 6, 7, 41], the solution of the metric structure is very complicated. Moreover, for finite temperature case, the temperature dependence of the dilaton potential is not obvious. In Ref.[44], instead of input the dilaton potential, we solve the dilaton

potential for given metric structure of deformed AdS<sub>5</sub> model, which can capture some features of QCD phenomenology at zero temperature. In this work, we will extend the minimal non-critical string framework to finite temperature, and investigate the phase transitions, the equation of state and the temperature dependence of loop operators.

## 2.2 Graviton-dilaton system with dual black-hole for hQCD model

The finite temperature dynamics of gauge theories, has a natural holographic counterpart in the thermodynamics of black-holes on the gravity side. Our holographic model is defined in the string frame, it is convenient to calculate the vacuum expectation value of the loop operator in the string frame, however it is more convenient to work out the gravity solution and study equation of state in the Einstein frame. Therefore, for later use, we will firstly derive the relation between the string frame and the Einstein frame.

If the metric in the Einstein frame  $g_{\mu\nu}^E$  and its corresponding metric structure in the string frame  $g_{\mu\nu}^S$  are connected by the scaling transformation

$$g_{\mu\nu}^S = e^{-2\Omega} g_{\mu\nu}^E, \quad (2.5)$$

then the scalar curvature in the Einstein frame and string frame has the following exact relationship:

$$e^{-2\Omega} R^S = R^E - (D-1)(D-2)\partial_\mu\Omega\partial^\mu\Omega + 2(D-1)\nabla^2\Omega, \quad (2.6)$$

with  $D$  the dimension, and  $\nabla^2$  is defined by  $\frac{1}{\sqrt{-g^E}}\partial_\mu\sqrt{-g^E}\partial^\mu$ , which is useful to derive the exact relation between two actions in string frame or Einstein frame.

In the case of  $D = 5$ , we have

$$\int \sqrt{-g^S} e^{m\Omega} R^S = \int \sqrt{-g^E} e^{(m-3)\Omega} [R^E - 12\partial_\mu\Omega\partial^\mu\Omega + 8(m-3)\nabla^2\Omega], \quad (2.7)$$

$$\int \sqrt{-g^S} e^{m\Omega} (g_S^{\mu\nu}\partial_\mu\Omega\partial_\nu\Omega) = \int \sqrt{-g^E} e^{(m-5)\Omega} (e^{2\Omega} g_E^{\mu\nu}\partial_\mu\Omega\partial_\nu\Omega). \quad (2.8)$$

The dilaton potentials in two different frames own the following relationship

$$V_S(\Omega) = V_E(\Omega)e^{2\Omega}. \quad (2.9)$$

By setting  $m = 3$  and  $\Omega = -\frac{2}{3}\phi$ , we have

$$V_S = V_E e^{\frac{-4\phi}{3}}, \quad (2.10)$$

and the following relation:

$$\begin{aligned} & \int \sqrt{-g^S} e^{-2\phi} (R^S + 4\partial_\mu\phi\partial^\mu\phi - V_S(\phi)) \\ &= \int \sqrt{-g^E} \left[ R^E - \frac{4}{3}\partial_\mu\phi\partial^\mu\phi - V_E(\phi) \right]. \end{aligned} \quad (2.11)$$

Therefore, Eq.(2.4) in the Einstein frame becomes:

$$S_{5D} = \frac{1}{16\pi G_5} \int d^5x \sqrt{-g^E} \left( R - \frac{4}{3} \partial_\mu \phi \partial^\mu \phi - V_E(\phi) \right) \quad (2.12)$$

Adding the black-hole background to the holographic QCD model constructed from vacuum properties, in the string frame we have

$$ds_S^2 = \frac{L^2 e^{2A_s}}{z^2} \left( -f(z) dt^2 + \frac{dz^2}{f(z)} + dx^i dx^i \right), \quad (2.13)$$

with  $L$  the radius of AdS<sub>5</sub>. The metric in the string frame is useful to calculate the loop operator. To derive the Einstein equations and to study the thermodynamical properties of equation of state, we transform it to the Einstein frame

$$ds_E^2 = \frac{L^2 e^{2A_s - \frac{4\phi}{3}}}{z^2} \left( -f(z) dt^2 + \frac{dz^2}{f(z)} + dx^i dx^i \right). \quad (2.14)$$

The general Einstein equations from the action (2.12) takes the form of:

$$E_{\mu\nu} + \frac{1}{2} g_{\mu\nu}^E \left( \frac{4}{3} \partial_\mu \phi \partial^\mu \phi + V_E(\phi) \right) - \frac{4}{3} \partial_\mu \phi \partial_\nu \phi = 0. \quad (2.15)$$

By using Eqs.(2.14) and (2.12), we can derive the following nontrivial Einstein equations in  $(t, t)$ ,  $(z, z)$  and  $(x_1, x_1)$  spaces, respectively:

$$\begin{aligned} & A_s''(z) + A_s'(z) \left( \frac{f'(z)}{2f(z)} - \frac{4}{3} \phi'(z) - \frac{2}{z} + A_s'(z) \right) - f'(z) \left( \frac{\phi'(z)}{3f(z)} + \frac{1}{2zf(z)} \right) \\ & - \frac{2\phi''(z)}{3} + \frac{2}{3} \phi'(z) \left( \phi'(z) + \frac{2}{z} \right) + \frac{L^2 V_E(\phi(z))}{6z^2 f(z)} e^{2A_s(z) - \frac{4\phi(z)}{3}} + \frac{2}{z^2} = 0 \end{aligned} \quad (2.16)$$

$$\begin{aligned} & \phi'(z)^2 - \phi'(z) \left( 4A_s'(z) + \frac{f'(z)}{2f(z)} - \frac{4}{z} \right) + A_s'(z) \left( \frac{3f'(z)}{4f(z)} - \frac{6}{z} + 3A_s'(z) \right) \\ & - \frac{3f'(z)}{4rf(z)} + \frac{3}{z^2} + \frac{L^2 V_E(\phi(z))}{4z^2 f(z)} e^{2A_s(z) - \frac{4\phi(z)}{3}} = 0 \end{aligned} \quad (2.17)$$

$$\begin{aligned} & f''(z) + \left( 6A_s'(z) - 4\phi'(z) - \frac{6}{z} \right) f'(z) + \frac{L^2 V_E(\phi(z))}{z^2} e^{2A_s(z) - \frac{4\phi(z)}{3}} \\ & + f(z) \left( 6A_s''(z) - \frac{4A_s'(z)(2z\phi'(z) + 3)}{z} + 6A_s'(z)^2 \right) \\ & + \frac{12}{z^2} - 4\phi''(z) + 4\phi'(z)^2 + \frac{8\phi'(z)}{z} = 0 \end{aligned} \quad (2.18)$$

One should notice that the above three equations are not independent. There are only two independent functions, one left equation is to check the consistence of the



solutions. To simplify the above equations, one can use the following two equations without dilaton potential  $V_E$ :

$$\begin{aligned}\phi''(z) - \left(2A'_s(z) - \frac{2}{z}\right) \phi'(z) - \frac{3A''_s(z)}{2} + \frac{3}{2}A'_s(z)^2 - \frac{3A'_s(z)}{z} &= 0, \\ f''(z) + \left(3A'_s(z) - 2\phi'(z) - \frac{3}{z}\right) f'(z) &= 0.\end{aligned}\quad (2.19)$$

The EOM of the dilaton field is given as following

$$\frac{8}{3}\partial_z \left( \frac{L^3 e^{3A_s(z)-2\phi} f(z)}{z^3} \partial_z \phi \right) - \frac{L^5 e^{5A_s(z)-\frac{10}{3}\phi}}{z^5} \partial_\phi V_E = 0. \quad (2.20)$$

For any holographic QCD model with given metric structure  $A_s(z)$  in the string frame, we can derive the general solutions to the Einstein equations, which take the following form:

$$\begin{aligned}\phi(z) &= \phi_0 + \phi_1 \int_0^z \frac{e^{2A_s(x)}}{x^2} dx + \frac{3A_s(z)}{2} \\ &\quad + \frac{3}{2} \int_0^z \frac{e^{2A_s(x)} \int_0^x y^2 e^{-2A_s(y)} A'_s(y)^2 dy}{x^2} dx, \\ f(z) &= f_0 + f_1 \left( \int_0^z x^3 e^{2\phi(x)-3A_s(x)} dx \right), \\ V_E(\phi) &= \frac{e^{\frac{4\phi(z)}{3}-2A_s(z)}}{L^2} \\ &\quad \left( z^2 f''(z) - 4f(z) \left( 3z^2 A''_s(z) - 2z^2 \phi''(z) + z^2 \phi'(z)^2 + 3 \right) \right).\end{aligned}\quad (2.21)$$

Where  $\phi_0, \phi_1, f_0, f_1$  are constants of integration. In Appendix A, we list several simple exact solutions of the Einstein equations by using Eq.(2.21).

### 3. Dual black-hole solution for the hQCD model with quadratic correction

From the experiences of constructing holographic QCD models for describing the heavy quark potential and the light hadron spectra, we have learnt that a quadratic background correction is related to the confinement property, i.e. the linear quark anti-quark potential and the linear Regge behavior. A positive quadratic correction,  $e^{cz^2}$  with  $c > 0$ , in the deformed warp factor of  $\text{AdS}_5$  can help to realize the linear heavy quark potential [35]. A quadratic dilaton background in the 5D meson action, whose effect in some sense looks like introducing a negative quadratic correction,  $e^{-cz^2}$ , in the warp factor of the  $\text{AdS}_5$  geometry, is helpful to realize the linear Regge behavior of hadron excitations [34].

Therefore, we introduce the following holographic QCD model with positive and negative quadratic correction in the deformed warp factor of AdS<sub>5</sub> in Eq.(2.13), i.e. we take

$$A_s(z) = ck^2z^2 \quad (3.1)$$

with  $c = \pm$  indicating the positive and negative quadratic correction, respectively. The main purpose in this section is to solve the dual black-hole background, corresponding dilaton field, and dilaton potential in the Graviton-dilaton system for the given hQCD model Eq.(3.1). To get the solution of equations Eq.(2.16)-Eq.(2.20), we impose the asymptotic AdS<sub>5</sub> condition  $f(0) = 1$  near the UV boundary  $z \sim 0$ , and require  $\phi, f$  to be finite  $z = 0, z_h$  with  $z_h$  the black-hole horizon. Fortunately, we find that the solution of the black-hole background takes the form of,

$$f(z) = 1 - f_c^h \int_0^{kz} x^3 \exp\left(\frac{3}{2}cx^2(H_c(x/k) - 1)\right) dx, \quad (3.2)$$

with

$$f_c^h = \frac{1}{\int_0^{kz_h} x^3 \exp\left(\frac{3}{2}cx^2(H_c(x/k) - 1)\right) dx}, \quad (3.3)$$

and

$$H_c(z) = {}_2F_2\left(1, 1; 2, \frac{5}{2}; 2ck^2z^2\right). \quad (3.4)$$

It is worthy of mentioning that in Ref.[10, 11, 12], the authors also investigated the thermodynamic properties of the deformed AdS<sub>5</sub> model with positive quadratic correction in the warp factor, however, there the black-hole background was not solved self-consistently from the graviton-dilaton system, but just taken from the AdS<sub>5</sub> Schwarz black-hole (AdS-SW BH) background

$$f(z) = 1 - z^4/z_T^4, \quad (3.5)$$

with  $z_T = 1/\pi T$ .

The solutions for the dilaton field and the dilaton potential take the forms as following:

$$\phi(z) = \frac{3}{4}ck^2z^2(1 + H_c(z)), \quad (3.6)$$

$$\begin{aligned} V_E^c(z) = & \frac{3e^{ck^2z^2(-1+H_c(z))}}{128L^2k^2z^2} \left(1 - f_c^h \int_0^{kz} e^{\frac{3}{2}cx^2(-1+H_c(\frac{x}{k}))} x^3 dx\right) [40k^2z^2 + \\ & 64ck^4z^4 - 384k^6z^6 + 12\sqrt{2\pi}e^{2ck^2z^2}kz(-7 + 20ck^2z^2)Er f_c(\sqrt{2}kz) \\ & - 27\pi e^{4ck^2z^2}Er f_c(\sqrt{2}kz)^2] - \\ & \frac{3f_c^h e^{\frac{5}{2}ck^2z^2(-1+H_c(z))}k^3z^3}{16L^2} [4kz - 16ck^3z^3 + 3\sqrt{2\pi}e^{2ck^2z^2}Er f_c(\sqrt{2}kz)] \end{aligned} \quad (3.7)$$

We have used  $V_E^\pm$  to represent the solution of the dilaton potential for  $c = \pm$ . Where the function  ${}_2F_2(\{a_1, \dots, a_p\}; \{b_1, \dots, b_q\}; z)$  is a generalized hypergeometric function which has series of  $\sum_{k=0}^{\infty} (a_1)_k \dots (a_p)_k / (b_1)_k \dots (b_q)_k z^k / k!$  and  $f_0$  is related to the integral constant which can be expressed by the position of the horizon of the black hole solution. The function  $Er f_c[z]$  appeared is also a special function class named by error function which is defined as integral form  $Er f_+[z] = Er f[z] = \frac{2}{\sqrt{\pi}} \int_0^z e^{-t^2} dt$  and  $Er f_-[z] = Er fi[z] = \frac{Er f[iz]}{i}$ .

Conformal invariance in the UV can be obtained when  $\phi \sim 0$  at the UV boundary  $z \rightarrow 0$ . One can expand  $\phi(z)$  at UV boundary  $z \sim 0$ ,

$$\phi(z \rightarrow 0) \sim \frac{3ck^2 z^2}{2} + \frac{3k^4 z^4}{10} + \dots \quad (3.8)$$

The behavior shown in Eq.(3.8) is consistent with the requirement of the asymptotic AdS<sub>5</sub> near the ultraviolet boundary.

Through the AdS/CFT dictionary, for any dilaton field  $\Phi$ , we have

$$\lim_{\Phi \rightarrow 0} V(\Phi) = -\frac{12}{L^2} + \frac{1}{2L^2} \Delta(\Delta - 4) \Phi^2 + O(\Phi^4). \quad (3.9)$$

By using the below relationship,

$$\partial_\Phi^2 V(\Phi) = \frac{\partial r}{\partial \Phi} \frac{\partial}{\partial r} \left( \frac{\partial r}{\partial \Phi} \frac{\partial V(z)}{\partial r} \right) = M_\Phi^2 \Phi^2 + \dots, \quad (3.10)$$

one can easily get the conformal dimension of the dilaton field near the UV boundary. In Eq. (3.9),  $\Delta$  is defined as  $\Delta(\Delta - 4) = M_\Phi^2 L^2$ , which is constrained by the Breitenlohner-Freedman (BF) bound  $2 < \Delta < 4$ . In our case,  $\Phi = \sqrt{\frac{8}{3}} \phi$ ,

$$M_\Phi^2 = -\frac{4}{L^2}, \quad (3.11)$$

for  $c = \pm$ . Therefore, the conformal dimension of the dilaton field is  $\Delta = 2$  in our holographic models with  $c = \pm$ , which satisfies the BF bound but does not correspond to any local, gauge invariant operator in 4D QCD. Although there have been some discussions in recent years of the possible relevance of a dimension two condensate in the form of a gluon mass term [47], it is not clear whether we can associate  $\phi$  with dimension-2 gluon condensate, because the *AdS/CFT* correspondence requires that bulk fields should be dual to gauge-invariant local operators.

#### 4. Equation of state for hQCD model with quadratic correction

A black-hole solution with a regular horizon is characterized by the existence of a surface  $z = z_h$ , where  $f(z_h) = 0$ . The Euclidean version of the solution is defined

only for  $0 < z < z_h$ , in order to avoid the conical singularity, the periodicity of the Euclidean time can be fixed by

$$\tau \rightarrow \tau + \frac{4\pi}{|f'(z_h)|}. \quad (4.1)$$

This determines the temperature of the solution as

$$T = \frac{|f'(z_h)|}{4\pi}. \quad (4.2)$$

From Eq. (3.2), one can easily read out the relation between the temperature and position of the black hole horizon.

$$T = \frac{k^4 z_h^3 \exp\left(\frac{3}{2}(ck^2 z_h^2 H_c(z_h) - ck^2 z_h^2)\right)}{4\pi \int_0^{kz_h} e^{\frac{3}{2}(-ck^2 x^2 + ck^2 x^2 H_c(x) + \text{Log}[k^2 x^2])} dx} \quad (4.3)$$

#### 4.1 The would-be critical temperature

According to Eq.(4.3), we cannot get the analytical expression to describe the relation between the temperature and horizon. The numerical results for the temperature as a function of the horizon  $z_h$  for  $c = +$  and  $c = -$  are shown in Fig.1 (a) and (b), respectively. Here we have taken  $k = 0.43\text{GeV}$ . The dashed lines are results from the pure AdS<sub>5</sub> Schwarz black-hole in Eq.(3.5).

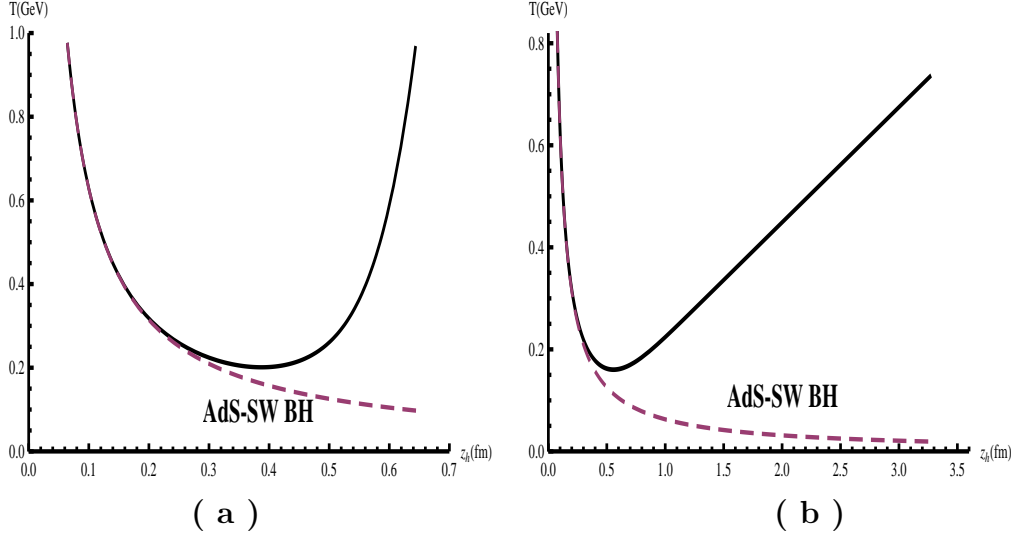


**Figure 1:** The temperature  $T$  as a function of the black-hole horizon  $z_h$  with  $k = 0.43\text{GeV}$  for  $c = +$  in (a) and  $c = -$  in (b), respectively. The dashed lines are for pure AdS<sub>5</sub> Schwarz black-hole.

From Fig. 1, it is noticed that for pure AdS<sub>5</sub> Schwarz black-hole, the temperature monotonically decreases with the increase of the horizon [10, 11, 12]. If one solves the

dual black-hole background self-consistently, one can find that for both hQCD models with positive and negative quadratic correction, there is a minimal temperature  $T_{min}$  at certain black-hole horizon  $z_h^0$ . This is similar to the case for the confining theory (at zero temperature) discussed in Ref. [6]. For  $T < T_{min}$ , there are no black-hole solutions. For  $T > T_{min}$ , there are two branches of black-hole solutions. When  $z_h < z_h^0$ , the temperature increases with the decreasing of  $z_h$ , which means that the temperature increases when the horizon moves close to UV, this phase is thermodynamically stable. When  $z_h > z_h^0$ , the temperature increases with the increase of  $z_h$ , which means that the temperature becomes higher and higher when the horizon moves to IR. This indicates that the solution for the branch  $z_h > z_h^0$  is unstable and thus not physical.

In order to determine the critical temperature, we have to compare the free energy difference between the stable black hole solution and the thermal gas. The thermal gas is solved by setting  $f_0(z) = 1$  [6, 48]. From the AdS/CFT conjecture, the gravity side is weakly coupled, so we can use the semi-classical approximation and just deal with the on-shell action. Following Ref. [48] and Appendix C in Ref. [6], the regularized total on-shell action in Euclidean space can be decomposed as three parts:

$$I^R = I_E^R + I_{GH}^R + I_{count}^R = I^\epsilon + I^{IR} + I^{count}, \quad (4.4)$$

with  $I_E^R$  the on-shell Einstein action,  $I_{GH}^R$  the Gibbons-Hawking term and  $I_{count}^R$  the counter term from the renormalization scheme.  $I^\epsilon$  and  $I^{IR}$  are the contributions at UV cut-off  $z = \epsilon$  and IR cut-off  $z = z_{IR}$ , respectively. Correspondingly, the free energy density is defined as

$$\mathcal{F} = \frac{T}{V_3} I^R = \mathcal{F}^\epsilon + \mathcal{F}^{IR} + \mathcal{F}^{count}, \quad (4.5)$$

with  $V_3$  the volume of the three-space.

To compare the free-energy density of the black-hole case and the thermal gas case, one has to impose the following conditions [49]:

$$\phi_0(z) |_{\epsilon=} = \phi(z) |_{\epsilon}, \quad (4.6)$$

$$\tilde{\beta} b_0(z) |_{\epsilon=} = \beta b(z) \sqrt{f(z)} |_{\epsilon}, \quad (4.7)$$

$$\tilde{V}_3 b_0^3(z) |_{\epsilon=} = V_3 b^3(z) |_{\epsilon}. \quad (4.8)$$

Where  $\phi_0, b_0, \tilde{\beta}, \tilde{V}_3$  are for thermal gas with  $b_0 = \frac{L}{z} e^{A_{E0}(z)}$  and  $A_{E0} = A_{s0} - \frac{2}{3}\phi_0$ , and  $\phi, b, \beta, V_3$  are for the black-hole with  $b(z) = \frac{L}{z} e^{A_E(z)}$ .

The free energy density for the black-hole has the form of

$$\mathcal{F}_{BH} = \mathcal{F}_{BH}^\epsilon + \mathcal{F}_{BH}^{count} \quad (4.9)$$

$$\mathcal{F}_{BH}^\epsilon = 2M^3 \left( 3b(\epsilon)^2 f(\epsilon) b'(\epsilon) + \frac{1}{2} b(\epsilon)^3 f'(\epsilon) \right), \quad (4.10)$$

where we have defined  $M^3 = 1/(16\pi G_5)$ . It is noticed that for black-hole case,  $z_{IR}$  is normally set at the horizon  $z_h$ , therefore  $I^{IR}$  vanishes due to  $f(z_h) = 0$ . At the limit  $\epsilon \rightarrow 0$ , we have

$$\mathcal{F}_{BH}^\epsilon = -\frac{6(L^3 M^3)}{\epsilon^4} - \left( \frac{6}{5} k^4 L^3 M^3 - \frac{1}{2} k^4 L^3 M^3 f_c^h \right) + o(\epsilon^2). \quad (4.11)$$

For detailed derivation of Eq.(4.11), please refer to Appendix B.

The free energy density for the thermal gas takes the form of

$$\mathcal{F}_{TG} = \mathcal{F}_{TG}^\epsilon + \mathcal{F}_{TG}^{IR} + \mathcal{F}_{TG}^{count}, \quad (4.12)$$

$$\mathcal{F}_{TG}^\epsilon = 2M^3 \frac{b(\epsilon)^4 \sqrt{f(\epsilon)}}{b_0(\epsilon)^4 \sqrt{f_0(\epsilon)}} \left( 3b_0(\epsilon)^2 f_0(\epsilon) b_0'(\epsilon) + \frac{1}{2} b_0(\epsilon)^3 f_0'(\epsilon) \right), \quad (4.13)$$

$$\mathcal{F}_{TG}^{IR} = 2M^3 f_0(z_{IR}) b_0^2(z_{IR}) b_0'(z_{IR}). \quad (4.14)$$

At the limit  $\epsilon \rightarrow 0$ , from the results derived in Appendix B, the free energy density of the thermal gas at UV cut-off takes the form of

$$\mathcal{F}_{TG}^\epsilon = -\frac{6L^3 M^3}{\epsilon^4} - \left( \frac{6}{5} k^4 L^3 M^3 - \frac{3}{4} k^4 L^3 M^3 f_c^h \right) + o(\epsilon^2). \quad (4.15)$$

Where we have used  $f_0(z) = 1$  in the derivation.

The divergent behaviors of the thermal gas and black-hole are the same, i.e, the counter terms  $\mathcal{F}_{BH}^{count}$  and  $\mathcal{F}_{TG}^{count}$  would have the same contribution in the two phases thus  $\mathcal{F}_{BH}^{count} - \mathcal{F}_{TG}^{count}$  would disappear in the free energy difference. Therefore, the final expression of the free energy difference has the form of

$$\Delta\mathcal{F} = \mathcal{F}_{BH} - \mathcal{F}_{TG} = -\frac{1}{4} k^4 M^3 L^3 f_c^h - 2M^3 b_0^2(z_{IR}) b_0'(z_{IR}). \quad (4.16)$$

It is worthy of mentioning that  $f_c^h > 0$ , therefore the contribution from the first term is always negative. Furthermore, from Eq.(B.15), we can observe that the first term contribution is exactly  $-\frac{1}{4}Ts$  with  $s$  the entropy density, and the free energy difference can be written as:

$$\Delta\mathcal{F} = -\frac{1}{4}Ts - 2M^3 b_0^2(z_{IR}) b_0'(z_{IR}). \quad (4.17)$$

Because  $b_0(z)$  is monotonically decreasing with  $z$  so  $b_0'(z) < 0$ , the second term contribution to the free energy difference is always positive. The expression of Eq.(4.17) is similar to Eq.(3.25) in Ref.[6]. We can observe that the second term contribution in Eq.(4.17) plays the same role of the gluon-condensate in Ref.[6].

The second term contribution in Eq.(4.17) is  $z_{IR}$  dependent. If we follow Ref.[6] and choose  $z_{IR}$  at the good singularity point, i.e,  $z_{IR} \rightarrow \infty$ , where  $b_0(z_{IR}) \rightarrow 0$ , then

the second term contribution in Eq.(4.16), i.e, the  $z_{IR}$  related term vanishes and we have

$$\Delta\mathcal{F} = \mathcal{F}_{BH} - \mathcal{F}_{TG} = -\frac{1}{4}k^4 M^3 L^3 f_c^h = -\frac{1}{4}Ts < 0. \quad (4.18)$$

This indicates that the black-hole phase is more stable than the thermal gas. The free energy difference for the case of  $z_{IR} \rightarrow \infty$  as a function of  $T/T_{min}$  is shown in Fig. 2. The solid lines indicate the stable black-hole solution, and the dashed lines are for the unstable black-hole phase. It is seen that  $\Delta\mathcal{F}$  jumps to a negative value at  $T_{min}$ , then decreases with the increase of the temperature. In this case, we observe a zeroth order phase transition at  $T_{min}$  due to the free energy discontinuity. By choosing the parameters  $k = 0.43\text{GeV}$  and  $G_5/L^3 = 1.26$ , the value of  $-\Delta\mathcal{F}/T^4$  approaches 1.5 at high temperature, which is similar to the lattice data of the pressure density for pure SU(3) gauge theory [25].

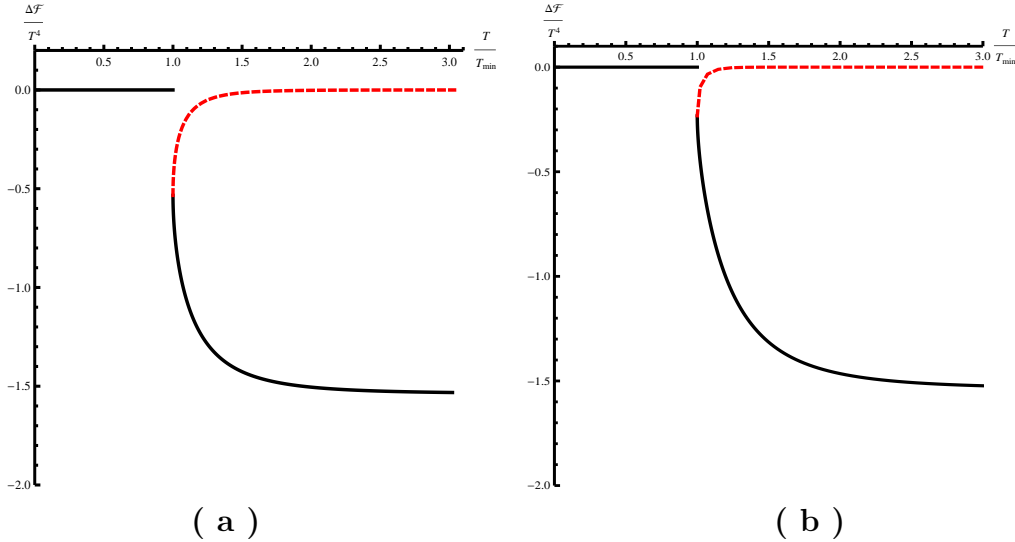


**Figure 2:** The free energy difference of Eq.(4.18) scaled by  $T^4$  as a function of  $T/T_{min}$  with  $k = 0.43\text{GeV}$  and  $G_5/L^3 = 1.26$  for  $c = +$  in (a) and  $c = -$  in (b), respectively. The dashed lines are for unstable black-hole solution.

In principle, the critical temperature  $T_c$  from Eq.(4.17) should be determined by finite value of  $z_{IR}$ , which sets the basic scale of the theory and should be fixed by experimental or lattice data. For example, for  $z_{IR} = 2.34\text{GeV}^{-1}$ , the free-energy difference will cross the zero-energy axis at  $T_{min}$  so that  $T_c = T_{min}$  and the phase transition will be of first order. If we choose other smaller value of  $z_{IR}$ , e.g,  $z_{IR} = 2\text{GeV}^{-1}$ , the free energy density difference will cross the zero-energy axis at  $T_c > T_{min}$  and the phase transition will be also of 1st order.

For our numerical calculations, we will firstly choose  $T_{min}(z_h^0)$  as the "would-be" critical temperature, which means that we choose a finite value of  $z_{IR} = 2.34\text{GeV}^{-1}$

and make  $\delta\mathcal{F} = 0$  at  $T_{min}$ . The exact thermal gas solution in the region  $T < T_{min}$  is unknown for us, therefore, we only focus on the temperature region  $T > T_{min}$  for the deconfined quark gluon plasma phase. In the following we will compare our results on the equation of state as a function of  $T/T_{min}$  with the lattice data as a function of  $T/T_c$ .

The value of  $T_{min}$  is only dependent on the model parameter  $k$  in Eq.(3.1). With given  $k = 0.43\text{GeV}$ , we can read the values of the critical temperature  $T_{min} = 201\text{MeV}$  and  $T_{min} = 160\text{MeV}$  for  $c = +$  and  $c = -$ , respectively. Both values are in agreement with lattice QCD result on the critical temperature [25, 26].

## 4.2 The entropy density

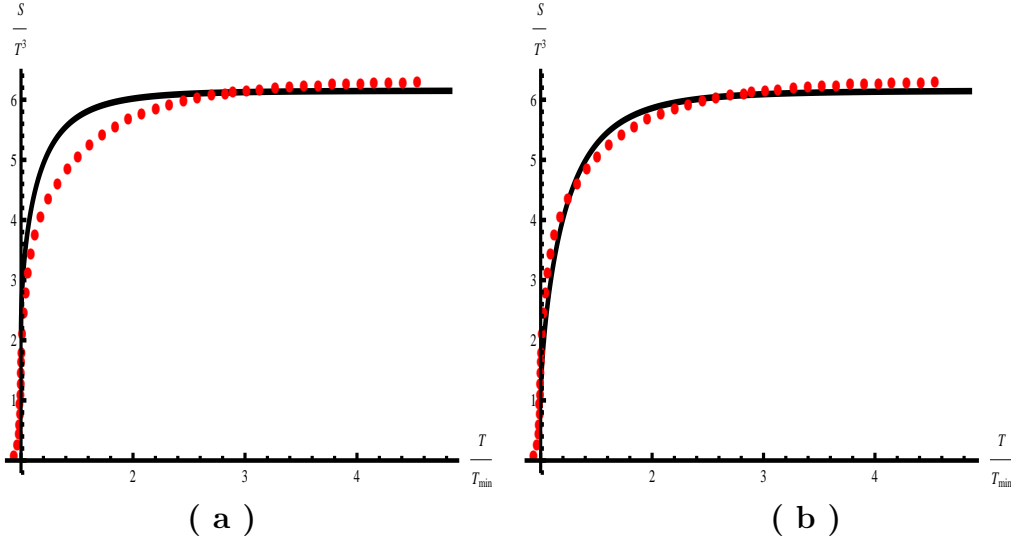


**Figure 3:** The scaled entropy density  $s/T^3$  as a function of scaled temperature  $T/T_{min}$  with  $k = 0.43\text{GeV}$  and  $G_5/L^3 = 1.26$  for  $c = +$  in (a) and  $c = -$  in (b), respectively. The dotted lines in (a) and (b) are lattice results as a function of  $T/T_c$  from [25].

Following the standard Bekenstein-Hawking formula [51], from the geometry given in Eq.(2.14), one can easily read the black-hole entropy density  $s$ , which is defined by the area  $A_{area}$  of the horizon:

$$s = \frac{A_{area}}{4G_5V_3} \Big|_{z_h} = \frac{L^3}{4G_5} \left( \frac{e^{A_s - \frac{2}{3}\phi}}{z} \right)^3 \Big|_{z_h}. \quad (4.19)$$

Where  $G_5$  is the Newton constant in 5D curved space and  $V_3$  is the volume of the spatial directions. It is noticed that the entropy density is closely related to the metric in the Einstein frame.

With fixed  $k = 0.43\text{GeV}$ ,  $G_5/L^3 = 1.26$ , the scaled entropy density  $s/T^3$  as a function of scaled temperature  $T/T_{min}$  is shown in Fig.3(a) for  $c = +$  ( $T_{min} =$



201MeV) and Fig.3(b) for  $c = -$  ( $T_{min} = 160\text{MeV}$ ), respectively. The dots in Fig.3 are the lattice result taken from [25]. It is can be seen that the entropy density in both positive and negative quadratic correction hQCD models agrees well with the lattice result for pure  $SU(3)$  gauge theory.

### 4.3 The pressure density, energy density and trace anomaly

The pressure density  $p(T)$  can be calculated from the entropy density  $s(T)$  by solving the equation

$$\frac{dp(T)}{dT} = s(T). \quad (4.20)$$

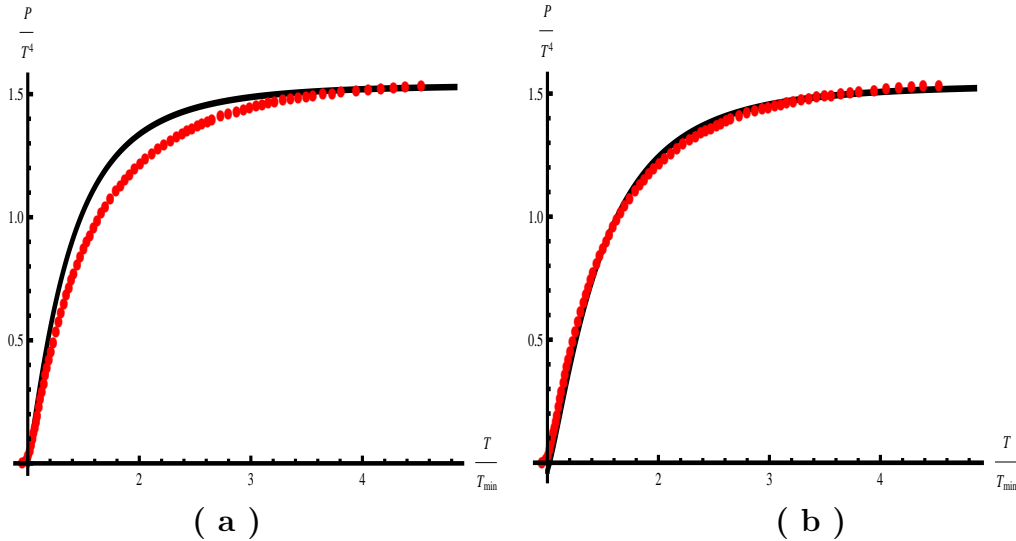


**Figure 4:** The scaled pressure density  $p/T^4$  as a function of scaled temperature  $T/T_{min}$  with  $k = 0.43\text{GeV}$  and  $G_5/L^3 = 1.26$  for  $c = +$  in (a) and  $c = -$  in (b), respectively. The dots are the lattice data as a function of  $T/T_c$  from [25].

After integrating the Bekenstein-Hawking entropy density, the pressure density of the system can be obtained up to a integral constant  $p_0$ . In our numerical calculation, we have set  $p_0 = 0$  to ensure  $p(T_{min}) = 0$ . In some sense, this procedure is equivalent to choose a finite value of  $z_{IR}$  in Eq.(4.17) to ensure  $\Delta\mathcal{F} = 0$  at  $T_{min}$ .

The numerical result of the pressure density as a function of temperature is shown in Fig.4. With fixed  $k = 0.43\text{GeV}$ ,  $G_5/L^3 = 1.26$ , the scaled pressure density  $p/T^4$  as a function of scaled temperature  $T/T_{min}$  is shown in Fig.4(a) for  $c = +$  ( $T_{min} = 201\text{MeV}$ ) and Fig.4(b) for  $c = -$  ( $T_{min} = 160\text{MeV}$ ), respectively. The dots in Fig.4 are the lattice result of pressure density for pure  $SU(3)$  gauge theory [25]. It can be seen that the pressure density in both hQCD models with  $c = \pm$  agree well with the lattice result.

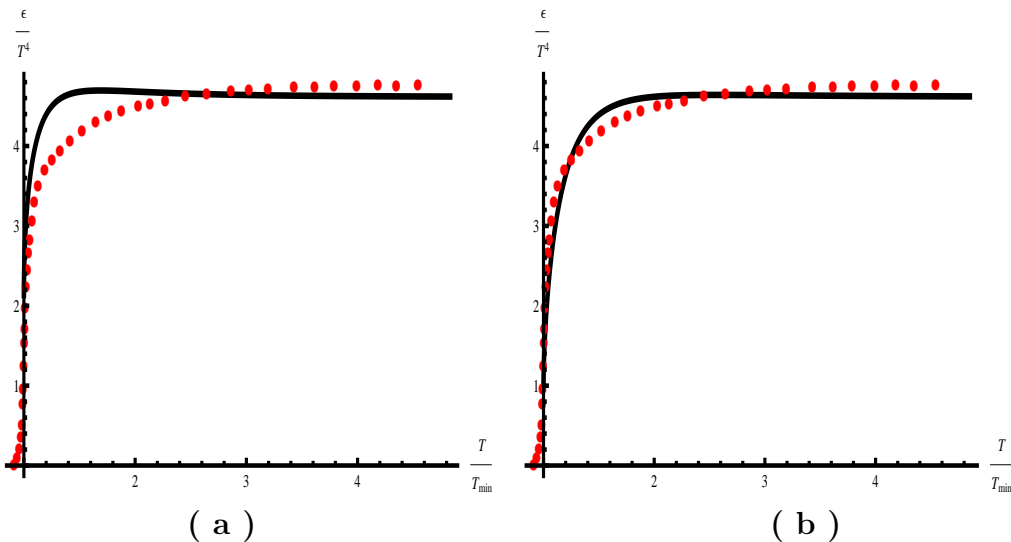


**Figure 5:** The scaled energy density  $\epsilon/T^4$  as a function of scaled temperature  $T/T_{min}$  with  $k = 0.43\text{GeV}$  and  $G_5/L^3 = 1.26$  for  $c = +$  in (a) and  $c = -$  in (b), respectively. The dots are lattice data as a function of  $T/T_c$  from [25].

Once we get the entropy density and pressure, we can get the energy density  $\epsilon$  immediately. The energy density is defined by

$$\epsilon = -p + sT. \quad (4.21)$$

The numerical result of energy density as a function of the temperature is shown in Fig.5. The lattice data for pure  $SU(3)$  gauge theory is shown with dots. It is found that the energy density from the two hQCD models with  $c = \pm$  agrees with the lattice data.

We also show the trace anomaly  $\epsilon - 3p$  in Fig.6. The trace anomaly shows a peak around  $T/T_{min} = 1.1$  for the case of  $c = +$  and  $T/T_{min} = 1.2$  for the case of  $c = -$ , and the height is around 3 for  $c = +$  and 2.5 for  $c = -$ . Both results are in agreement with lattice result. At very high temperature, the trace anomaly goes to zero, which indicates the system is asymptotically conformal at high temperature.

#### 4.4 The sound velocity and specific heat

The sound velocity  $c_s^2$  can be obtained from the temperature and entropy:

$$c_s^2 = \frac{d \log T}{d \log s} = \frac{s}{T ds/dT}, \quad (4.22)$$

which can directly measure the conformality of the system. For conformal system,  $c_s^2 = 1/3$ , for non-conformal system,  $c_s^2$  will deviate from  $1/3$ . From Eq.(4.22), we can see that the speed of the sound is independent of the normalization of the 5D Newton constant  $G_5$  and the space volume  $V_3$ .

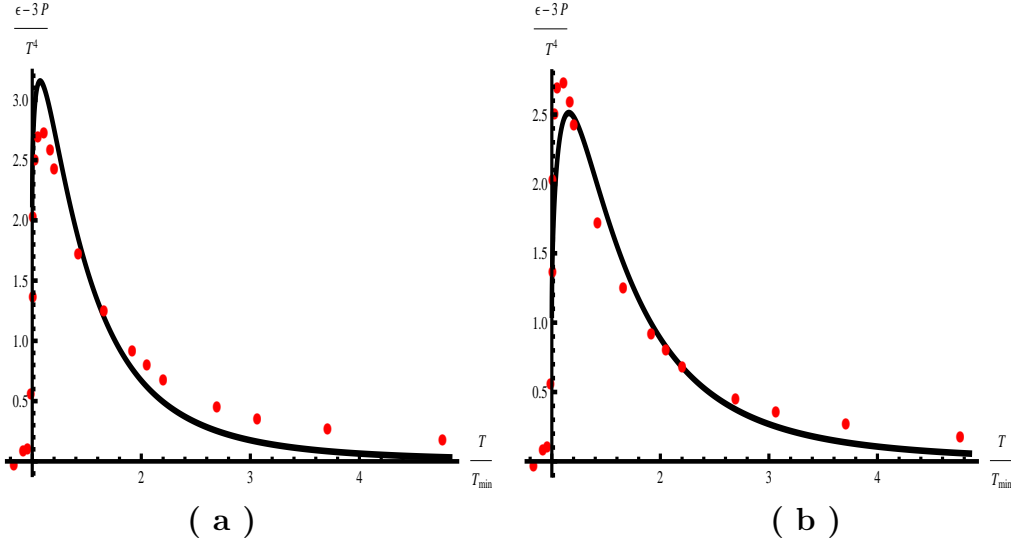


**Figure 6:** The trace anomaly  $\epsilon - 3p$  as a function of scaled temperature  $T/T_{min}$  with  $k = 0.43\text{GeV}$  and  $G_5/L^3 = 1.26$  for  $c = +$  in (a) and  $c = -$  in (b), respectively. The dots are the lattice data as a function of  $T/T_c$  from [25].

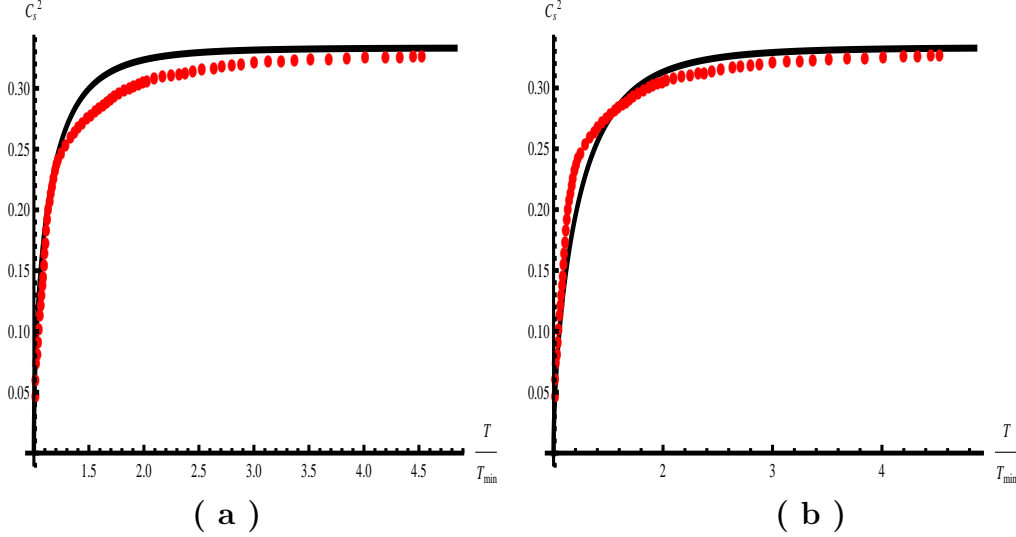


**Figure 7:** The square of the sound velocity  $c_s^2$  as a function of scaled temperature  $T/T_{min}$  with  $k = 0.43\text{GeV}$  and  $G_5/L^3 = 1.26$  for  $c = +$  ( $T_{min} = 201\text{MeV}$ ) and  $c = -$  ( $T_{min} = 160\text{MeV}$ ), respectively. The dotted line is the lattice data as a function of  $T/T_c$  from [25].

With known entropy density and the speed of sound, the specific heat  $C_v$  can be derived straightforwardly and takes the following expression:

$$C_v = \frac{d\epsilon}{dT} = T \frac{ds}{dT} = s/c_s^2. \quad (4.23)$$

At phase transition, the specific heat shows a clear  $\lambda$ -type anomaly or divergent

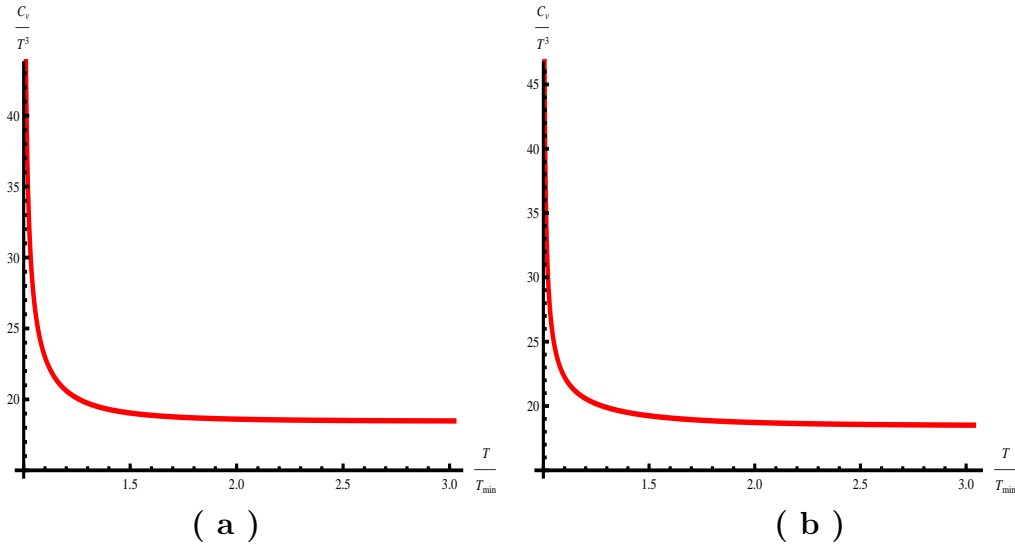


**Figure 8:** The scaled specific heat  $C_v/T^3$  as a function of scaled temperature  $T/T_{min}$  with  $k = 0.43\text{GeV}$  and  $G_5/L^3 = 1.26$  for  $c = +$  ( $T_{min} = 201\text{MeV}$ ) and  $c = -$  ( $T_{min} = 160\text{MeV}$ ), respectively.

behavior [52], which is consistent with the jump or fast change of entropy density at  $T_c$ . Therefore, it can be used to determine the phase transition point. At very high temperature, the specific heat for the free gas of pure gauge  $SU(N_c)$  theory has the relation [53]

$$C_v/T^3 = 4\epsilon/T^4 \rightarrow 4(N_c^2 - 1)\pi^2/15, \quad (4.24)$$

and at large  $N_c$  limit [6], it takes the limit of

$$C_v/T^3 \rightarrow 4N_c^2\pi^2/15. \quad (4.25)$$

The numerical result of the square of the sound velocity is shown in Fig.7. At  $T_{min}$ , the sound velocity square is around 0.05 for  $c = +$  and 0.02 for  $c = -$ , both are in agreement with lattice data 0.05. At high temperature, the sound velocity square goes to  $1/3$ , which means that the system is asymptotically conformal. The numerical result of the specific heat is shown in Fig.8. It can be clearly seen that the specific heat  $C_v$  diverges at  $T_{min}$ . At  $T \rightarrow \infty$ , we can see that the scaled specific heat  $C_v/T^3$  approaches the free gas limit of pure gluon system  $4(N_c^2 - 1)\pi^2/15$  with  $N_c = 3$ .

#### 4.5 Discussion

In this section, we have investigated the equation of state for two hQCD models with positive/negative quadratic correction in the deformed warp factor of  $\text{AdS}_5$ . It has been found that for both models, if we choose  $T_c = T_{min}$ , the properties of entropy density, pressure density, energy density and sound velocity are all in agreement with

lattice results for pure  $SU(3)$  gauge theory. As we have mentioned,  $T_c$  can be larger than  $T_{min}$ . By comparing our numerical results with lattice data, it is observed that to fit the lattice data well,  $T_c$  should be located in a neighborhood of  $T_{min}$  from above, which means  $z_{IR}$  should be in a neighborhood of  $z_{IR} = 2.34\text{GeV}^{-1}$  from below. If  $T_c$  lies in this small region around  $T_{min}$ , the numerical results on equation of state can fit lattice data almost equally well as that at  $T_c = T_{min}$ . It is worthy of mentioning that in our work choosing  $T_c = T_{min}$  can fit lattice data better. Therefore, we identify  $T_{min}$  as  $T_c$  in this work, and we believe that the qualitative results are not dependent on the exact location of  $T_c$ .

## 5. Heavy quark potential, Polyakov loop, spatial string tension at finite temperature

QCD vacuum is characterized by spontaneous chiral symmetry breaking and color confinement. The dynamical chiral symmetry breaking is due to a non-vanishing quark anti-quark condensate,  $\langle \bar{q}q \rangle \simeq (250\text{MeV})^3$  in the vacuum, which induces the presence of the light Nambu-Goldstone particles, the pions and kaons in the hadron spectrum. The confinement represents that only colorless states are observed in the spectrum, which is commonly described by the linearly rising potential between two heavy quarks at large distances,  $V_{\bar{Q}Q}(r) = \sigma r$ , where  $r$  is the distance between quark anti-quark, and  $\sigma \simeq (425\text{MeV})^2$  is the string tension of the flux tube.

It is expected that chiral symmetry can be restored and color degrees of freedom can be freed at high temperature and/or density. The chiral restoration and deconfinement phase transitions are characterized by the breaking and restoration of chiral and center symmetry, which are only well defined in two extreme quark mass limits, respectively. In the chiral limit when the current quark mass is zero  $m = 0$ , the chiral condensate  $\langle \bar{q}q \rangle$  is the order parameter for the chiral phase transition. When the current quark mass goes to infinity  $m \rightarrow \infty$ , QCD becomes pure gauge  $SU(3)$  theory, which is center symmetric in the vacuum, and the usually used order parameter is the Polyakov loop expectation value  $\langle L \rangle$  [54], which is related to the heavy quark free energy.

In Sec.4, we have investigated thermodynamic properties of two deformed  $AdS_5$  models with quadratic corrections, and have found that both models agree well with lattice results for pure  $SU(3)$  gauge theory. Therefore, we will not discuss the chiral phase transitions, but focus on deconfinement phase transition properties of these two models. In this section, we study the heavy quark potential, the Polyakov loop and the spatial Wilson loop at finite temperature, which are quantities related to deconfinement properties. It is worthy of mentioning that till now there is no good method to calculate the properties of these loop operators in the whole temperature region within the framework of field theory, though chiral phase transition can

be described by using effective QCD models, e.g. the Nambu–Jona-Lasinio (NJL) model [55] and the linear sigma model [56]. The gauge/gravity duality offers a non-perturbative method to calculate the loop operators, in return, lattice QCD results [57, 58, 59] of these loop operators will judge the validity of the hQCD model.

At last, we want to mention that all the quantities of loop operator will be calculated in the string frame, which is different from the way of calculating the thermal quantities for equation of state. In order to avoid confusion and also to keep this section self-contained, we explicitly list the metric and the solved dual black-hole background from Sec.3, which will be used in this section:

$$\begin{aligned} ds_S^2 &= \frac{L^2 e^{2A_s}}{z^2} \left( -f(z) dt^2 + \frac{dz^2}{f(z)} + dx^i dx^i \right), \\ A_s &= ck^2 z^2, \\ f(z) &= 1 - f_c \int_0^{kz} x^3 \exp\left(\frac{3}{2} cx^2 (H_c(x/k) - 1)\right) dx, \end{aligned} \quad (5.1)$$

with  $c = \pm$ , and  $f_c$  and  $H_c$  defined in Eq.(3.3) and (3.4), respectively.

### 5.1 The heavy quark potential

We firstly study the heavy quark potential. The linear heavy quark anti-quark potential normally indicates the confinement of quarks in the vacuum. Above the deconfinement critical temperature  $T_c$ , it is expected that the linear potential vanishes and the Coulomb potential to be exponentially screened at large distance. The heavy quark potential at finite temperature has been analyzed in lattice QCD [57].

In the framework of gauge/gravity duality, we follow the standard procedure [60] and [61] to derive the static heavy quark potential  $V_{Q\bar{Q}}(r)$  under the general metric background with a black hole, i.e, Eq. (5.1). In  $SU(N)$  gauge theory, the interaction potential for infinity massive heavy quark antiquark is calculated from the Wilson loop

$$W[C] = \frac{1}{N} \text{Tr} P \exp[i \oint_C A_\mu dx^\mu], \quad (5.2)$$

where  $A_\mu$  is the gauge field, the trace is over the fundamental representation,  $P$  stands for path ordering.  $C$  denotes a closed loop in space-time, which is a rectangle with one direction along the time direction of length  $T$  and the other space direction of length  $R$ . The Wilson loop describes the creation of a  $Q\bar{Q}$  pair with distance  $r$  at some time  $t_0 = 0$  and the annihilation of this pair at time  $t = T$ . For  $T \rightarrow \infty$ , the expectation value of the Wilson loop behaves as  $\langle W(C) \rangle \propto e^{-TV_{Q\bar{Q}}}$ . According to the *holographic* dictionary, the expectation value of the Wilson loop in four dimensions should be equal to the string partition function on the modified AdS<sub>5</sub> space, with the string world sheet ending on the contour  $C$  at the boundary of AdS<sub>5</sub>

$$\langle W^{4d}[C] \rangle = Z_{string}^{5d}[C] \simeq e^{-S_{NG}[C]}, \quad (5.3)$$

where  $S_{NG}$  is the classical world sheet Nambu-Goto action

$$S_{NG} = \frac{1}{2\pi\alpha_q} \int d^2\eta \sqrt{\text{Det}\chi_{ab}}, \quad (5.4)$$

with  $\alpha_q$  the string tension which has dimension of  $\text{GeV}^{-2}$ , and  $\chi_{ab}$  is the induced worldsheet metric with  $a, b$  the indices in the  $(\eta^0 = t, \eta^1 = x)$  coordinates on the worldsheet.

We consider the following situation there are static quark and ant-quark linked by one string. The position of one quark is  $x = -\frac{r}{2}$  and the other is  $x = \frac{r}{2}$ . Under the background (5.1), we can obtain the equation of motion:

$$\frac{\sqrt{f(z)}}{z^2} \frac{e^{2A_s(z)}}{\sqrt{1 + \frac{(z')^2}{f(z)}}} = \text{Constant} = \sqrt{f_0} \frac{e^{2A_s(z_0)}}{z_0^2}, \quad (5.5)$$

Here the  $r$  is dependent on  $z_0$  which is the maximal value of  $z$  and  $z'(x=0) = 0$ . In eq.(5.5), we have defined  $f_0 = f(z = z_0)$ . For the configuration mentioned above and the given equation of motion, we impose the following boundary conditions  $z(x=0) = z_0, z(x = \pm\frac{r}{2}) = 0$ . Following the standard procedure, one can derive the interquark distance  $r$  as a function of  $z_0$

$$r(z_0) = \int_0^1 d\nu \frac{2z_0\nu^2}{\sqrt{1 - \frac{f_0}{f(\nu z_0)} \nu^4 \frac{e^{4A_s(z_0)}}{e^{4A_s(z_0\nu)}}}} \frac{\sqrt{f_0}}{f(z_0\nu)} \frac{e^{2A_s(z_0)}}{e^{2A_s(z_0\nu)}}. \quad (5.6)$$

The heavy quark potential can be worked out from the Nambu-Goto string action:

$$V_{Q\bar{Q}}(z_0) = \frac{g_q}{\pi z_0} \int_0^1 d\nu \frac{1}{\sqrt{1 - \frac{f_0}{f(\nu z_0)} \nu^4 \frac{e^{4A_s(z_0)}}{e^{4A_s(z_0\nu)}}}} \frac{e^{2A_s(z_0\nu)}}{\nu^2}, \quad (5.7)$$

with  $g_q = \frac{L^2}{\alpha_q}$ . It is noticed that the integral in Eq.(5.7) in principle include some poles, which induces  $V_{Q\bar{Q}}(z) \rightarrow \infty$ . The infinite energy should be extracted through certain regularization procedure. The divergence of  $V_{Q\bar{Q}}(z)$  is related to the vacuum energy for two static quarks. Generally speaking, the vacuum energy of two static quarks will be different in various background. In our latter calculations, we will use the regularized  $V_{Q\bar{Q}}^{ren.}$ , which means the vacuum energy has been subtracted.

Fig.9 shows the heavy quark potential  $V_{Q\bar{Q}}/g_q$  as a function of the distance between the two static quarks  $r$  for different temperatures  $T/T_{min} = 1, 1.5, 2, 2.5, 3$ . Fig.9(a) is for  $c = +$ , i.e, the positive quadratic correction model, and Fig.9(b) is for  $c = -$ , i.e, the negative quadratic correction model. For  $c = +$ , the heavy quark potential has a linear part at zero temperature as shown in Ref. [44]. It is observed that when  $T > T_{min}$ , the linear part vanishes, and with the increases of the temperature, the Coulomb part potential gets screened. This picture qualitatively

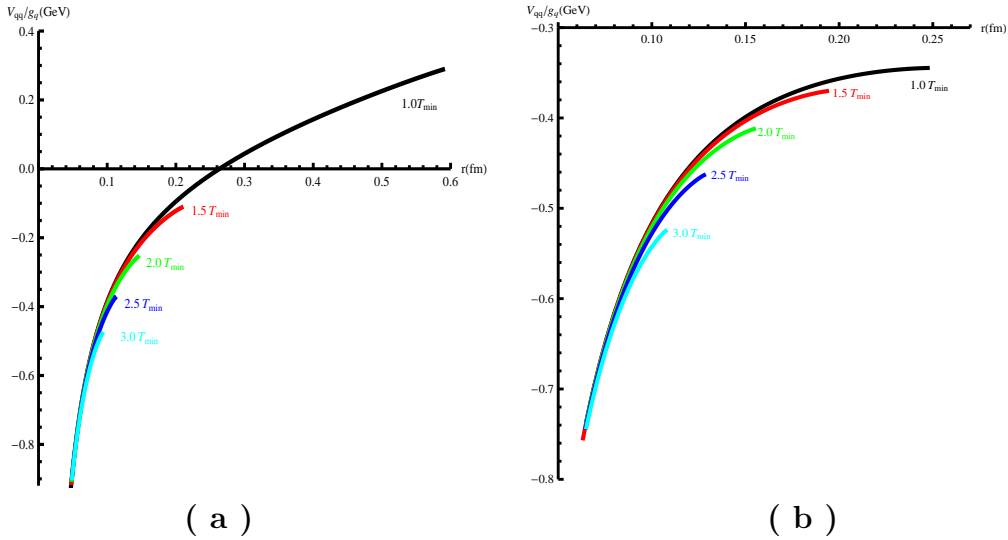


**Figure 9:** The heavy quark potential  $V_{Q\bar{Q}}/g_q$  as a function of the separation distance  $r$  for different temperatures for  $c=+$  (a) and  $c=-$  (b), respectively. Where  $k = 0.43\text{GeV}$  is used.

agrees with lattice result in Ref. [57]. For the case of  $c=-$ , the heavy quark potential has no linear part at zero temperature as shown in Ref. [44]. It is seen that when  $T/T_{min} > 1$ , the heavy quark potential only contains Coulomb part, with the increase of the temperature, the Coulomb part gets screened.

We can see that, even though the heavy quark potential for hQCD models with positive and negative correction are quite different in the vacuum, the behavior of the heavy quark potential in these two hQCD models are qualitative the same above the critical temperature  $T_c$ . The imaginary part of the heavy quark potential at finite temperature in the framework of AdS/CFT has been discussed in Ref. [62].

## 5.2 The Polyakov loop

The Polyakov loop is defined as

$$L(T) = \frac{1}{N} \text{tr} P \exp \left[ ig \int_0^{1/T} dt A_0 \right], \quad (5.8)$$

where  $N$  is the colors, the trace is evaluated in the fundamental representation and  $P$  stands for the path ordering. In QCD with infinitely heavy quarks, the Polyakov loop is related to the operator that generates a static quark [54]. We can interpret the logarithm of the expectation value  $\langle L(T) \rangle$  as half of the free energy  $F_{Q\bar{Q}}$  of a static quark-anti-quark pair at infinite distance. The Polyakov loop is an order parameter for center symmetry of the gauge group. In the confined phase, the  $F_{Q\bar{Q}} \rightarrow \infty$ , which ensures  $\langle L(T) \rangle = 0$ , and thus the confined phase is center symmetric. The



deconfined phase is characterized by  $F_{Q\bar{Q}} < \infty$  and  $\langle L(T) \rangle \neq 0$ , which implies the center symmetry is breaking in the ordered phase.

In the framework of gauge/gravity duality, the Polyakov loop is the Wilson loop wrapping the periodic imaginary time direction [63]. This operator should be computed in the string frame [64]. We follow the method in Ref. [12] to calculate the expectation value of the Polyakov loop, which is schematically given by the world-sheet path integral

$$\langle L(T) \rangle = \int DX e^{-S_w}, \quad (5.9)$$

where  $X$  denotes a set of world-sheet fields.  $S_w$  is a world-sheet action. In principle, the integral (5.9) can be evaluated approximately in terms of minimal surfaces that obey the boundary conditions. The result is written as  $\langle L(T) \rangle = \sum_n w_n \exp[-S_n]$ , where  $S_n$  means a renormalized minimal area whose weight is  $w_n$ .

Given the background in the string frame Eq.(5.1), we can calculate the expectation value of the Polyakov loop by using the Nambu-Goto action for  $S_w$

$$S_{NG} = \frac{1}{2\pi\alpha_p} \int d^2\eta \sqrt{\text{Det}\chi_{ab}}, \quad (5.10)$$

with  $\alpha_p$  the string tension and  $\chi_{ab}$  the induced worldsheet metric with  $a, b$  the indices in the  $(\eta^1 = t, \eta^2 = z)$  coordinates on the worldsheet. It is noticed that here we have introduced a different string tension from that in Eq.(5.4). This can be understood that along different direction, the string tension is different. We will also introduce another different string tension parameter for the spatial Wilson loop. This yields

$$S_{NG} = \frac{g_p}{\pi T} \int_0^{z_h} dr \frac{e^{2A_s}}{z^2} \sqrt{1 + f(z)(\vec{x}')^2}, \quad (5.11)$$

where  $g_p = \frac{L^2}{2\alpha_p}$ . A prime stands for a derivative with respect to  $z$ .

The equation of motion for  $\vec{x}$  takes the form of

$$\left[ \frac{e^{2A_s}}{z^2} f(z) \vec{x}' / \sqrt{1 + f(z)(\vec{x}')^2} \right]' = 0. \quad (5.12)$$

The above equation has a special solution  $\vec{x} = \text{const}$ . Substituting this constant solution to Eq.(5.11), one can get the minimal world-sheet,

$$\begin{aligned} S_0 &= S'_0 + c_p, \\ S'_0 &= \frac{g_p}{\pi T} \int_0^{z_h} dz \left( \frac{e^{2A_s}}{z^2} - \frac{1}{z^2} \right). \end{aligned} \quad (5.13)$$

Where  $c_p$  is the normalization constant which is dependent on the scheme of the regularization procedure. It is noticed that Eq.(5.13) takes the same form as that in [12],

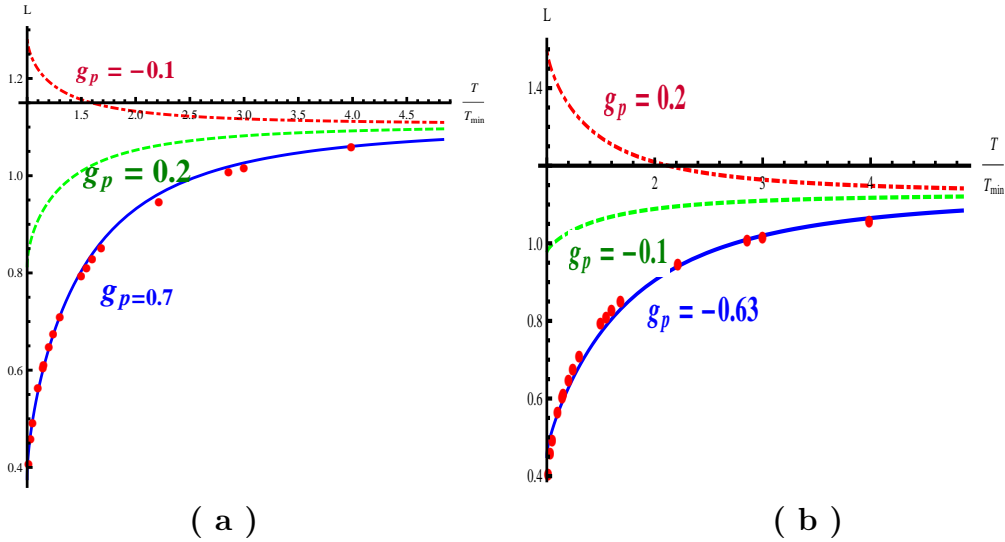


**Figure 10:** The expectation value of the Polyakov loop as a function of the temperature  $T/T_{min}$ : (a) in the case of  $c = +$  with  $k = 0.43\text{GeV}$ ,  $C_p = 0.1$  and  $g_p = -0.1, 0.2, 0.7$ , (b) in the case of  $c = -$  with  $k = 0.43\text{GeV}$ ,  $C_p = 0.12$ , and  $g_p = 0.2, -0.1, -0.63$ . The dots are lattice data as a function of  $T/T_c$  taken from [58].

where the black-hole background is taken from pure  $\text{AdS}_5$ . Therefore, Performing the integral over  $z$ , we get the same analytic expression as in [12]:

$$S'_0 = \frac{g_p}{\pi T} \frac{\sqrt{2\pi} k z_h \text{Erfi}(\sqrt{2} k z_h) - e^{2k^2 z_h^2} + 1}{z_h}, \quad c = +, \quad (5.14)$$

$$S'_0 = \frac{g_p}{\pi T} \frac{-\sqrt{2\pi} k z_h \text{Erf}(\sqrt{2} k z_h) - e^{-2k^2 z_h^2} + 1}{z_h}, \quad c = -. \quad (5.15)$$

Combining the weight factor with the normalization constant as  $C_p = \ln w_0 - c_p$ , we find

$$\langle L(T) \rangle = \exp \left\{ C_p - S'_0 \right\}. \quad (5.16)$$

The numerical result of the expectation value of the Polyakov loop as a function of the scaled temperature  $T/T_c$  is shown in Fig. 10 (a) and (b) for positive and negative quadratic correction models, respectively. The dots are lattice data taken from Ref.[58]. For the positive quadratic correction model, i.e,  $c = +$ , the parameters  $k = 0.43\text{GeV}$  and  $C_p = 0.1$  have been used for numerical calculation. We plot the Polyakov loop as a function of temperature for several values of  $g_p = -0.1, 0.2, 0.7$ , it is found that  $g_p = 0.7$  can remarkably fit the lattice data [58] for the pure  $SU(3)$  gauge theory. For the negative quadratic correction model, i.e,  $c = -$ , the parameters  $k = 0.43\text{GeV}$  and  $C_p = 0.12$  have been used for numerical calculation. We plot the Polyakov loop as a function of the temperature for several values of  $g_p = 0.2, -0.1, -0.63$ , it is observed that  $g_p = -0.63$  can fit the lattice result quite well.

It can be seen that both models by choosing different parameters can agree well with the lattice result on the Polyakov loop. However, we have to point out that in the case of  $c = -$ , a negative value  $g_p = -0.63$  has been taken to fit the lattice data. This means the string tension  $\alpha_p$  introduced in Eq.(5.10) is negative, which is not physical. Therefore, from the result of the expectation value of the Polyakov loop, the negative quadratic correction model can be excluded. Our result of the Polyakov loop for positive quadratic correction model fits lattice data remarkably.

### 5.3 The spatial Wilson loop

We now move on to discuss the spatial Wilson loop in the framework of the gauge/gravity duality.

The non-Abelian gauge theories undergo a deconfining phase transition at high temperature. The physical string tension, characterizing the linear rise of the potential between static quark sources with distance, decreases with increasing temperature and vanishes above  $T_c$ . The potential becomes a Debye screened Coulomb potential in the high temperature phase, which is shown in Sec.5.1. However, the phase just above  $T_c$  is more complicated than a weakly coupled quark gluon gas because of the appearance of some non-perturbative soft modes, e.g, the Debye screening mass  $m_D \sim gT$  and the magnetic screening mass  $m_M \sim g^2T$ . The soft mode in magnetic sector cannot be handled in any perturbative scheme. It is found that the non-perturbative physics arising from the magnetic sector reflects the survival of the area law behavior for space-like Wilson loops, i.e. confinement of magnetic modes. The spatial string tension,  $\sigma_s$ , extracted from the area law behavior of spatial Wilson loops, has been studied in lattice calculations [25, 59], and shows the expected dependence on the magnetic scale  $\sqrt{\sigma_s} \sim g^2(T)T$ .

In the framework of gauge/gravity duality, to calculate the spatial Wilson loop, we consider a rectangular loop  $\mathcal{C}$  along two spatial directions  $(x, y)$  [10]. The loop  $\mathcal{C}$  should wrap around the  $\mathcal{S}^1$  which is a circle in the time direction. The expectation value of the loop can be calculated through the following AdS/CFT dictionary:

$$V_s = \int DX e^{-S_w}. \quad (5.17)$$

Here  $X$  is the series of world sheet fields and  $S_w$  stands for a world sheet action. Again, at large  $N$ , the saddle point approximation is valid, and we only need to take the minimum value of the Euclidean action among the saddle points. In fact, given the boundary conditions, there will be UV divergence from the field theory viewpoint. It is necessary to regularize and make it finite by a divergent subtraction by introducing a counterterm.

Given the background in the string frame Eq.(5.1), we can calculate the expectation value of the spatial Wilson loop by using the Nambu-Goto action for  $S_w$

$$S_{NG} = \frac{1}{2\pi\alpha'} \int d^2\eta \sqrt{\text{Det}\chi_{ab}}, \quad (5.18)$$

with  $\alpha'$  the string tension and  $\chi_{ab}$  the induced worldsheet metric with  $a, b$  the indices in the  $(\eta^1 = x, \eta^2 = y)$  coordinates on the worldsheet. We take one of the spatial direction  $Y$  goes to infinity. The quark and anti-quark are set at  $x_i = \pm r/2$ , we can get the Nambu-Goto action as

$$S = \frac{g_{sv}}{2\pi} Y \int_{-r/2}^{r/2} dx \frac{h}{z^2} \sqrt{1 + \frac{z'^2}{f(z)}}, \quad (5.19)$$

here  $r$  stands for the separation between the static quark pair and  $g_{sv} = \frac{L^2}{\alpha'}$ . From the (5.19), one can easily get the equation of motion for  $x$ :

$$zz'' + (f(z) + z'^2) (2 - z\partial_z \ln h) - \frac{1}{2}z(z')^2 \partial_z \ln f(z) = 0. \quad (5.20)$$

Following the standard procedure, one can obtain the simple equation:

$$\frac{h}{z^2 \sqrt{1 + \frac{z'^2}{f(z)}}} = \frac{h_0}{z_0^2}. \quad (5.21)$$

Where  $h(z) = e^{2A_s(z)}$  and  $h_0 = h(z_0)$ . From the equation of motion, one can see that

$$r(z_0) = z_0 \int_0^1 \frac{2\nu^2 e^{-2ck^2(\nu^2-1)z_0^2}}{\sqrt{f(z_0\nu) (1 - \nu^4 e^{-4ck^2(\nu^2-1)z_0^2})}} d\nu, \quad (5.22)$$

where  $z_0 = z(x=0)$  which defined by  $z'(x=0) = 0$  is the maximum value of  $z$ . The free energy can be read:

$$S_{xy}(z_0) = \frac{g_{sv}}{\pi z_0} \int_0^1 \frac{e^{2ck^2\nu^2 z_0^2}}{\nu^2 \sqrt{f(z_0\nu) (1 - \nu^4 e^{-4ck^2(\nu^2-1)z_0^2})}} d\nu. \quad (5.23)$$

After subtracting the UV divergence, one can get the area of the two dimensional minimal surface given by the classical configuration of the Nambu-Goto action Eq.(5.21), and the regularized spatial Wilson loop has the following form:

$$V_s(z_0) = \frac{g_{sv}}{\pi z_0} \left( \int_0^1 \frac{1}{\nu^2} \left( \frac{e^{2ck^2\nu^2 z_0^2}}{\sqrt{f(z_0\nu) (1 - \nu^4 e^{-4ck^2(\nu^2-1)z_0^2})}} - 1 \right) d\nu - 1 \right). \quad (5.24)$$

Fig. 11 shows the regularized spatial potential  $V_s$  as a function of the distance between quark anti-quark  $r$  for several temperatures above  $T_{min}$ . For both  $c = +$  and  $c = -$  cases, the parameter  $k = 0.43\text{GeV}$  is used. It is found that for positive quadratic correction model, the spatial heavy quark potential always have a linear potential, and the slope of the linear potential increases with the temperature. This picture is in agreement with lattice result [25, 59]. For the case of  $c = -$ , the spatial

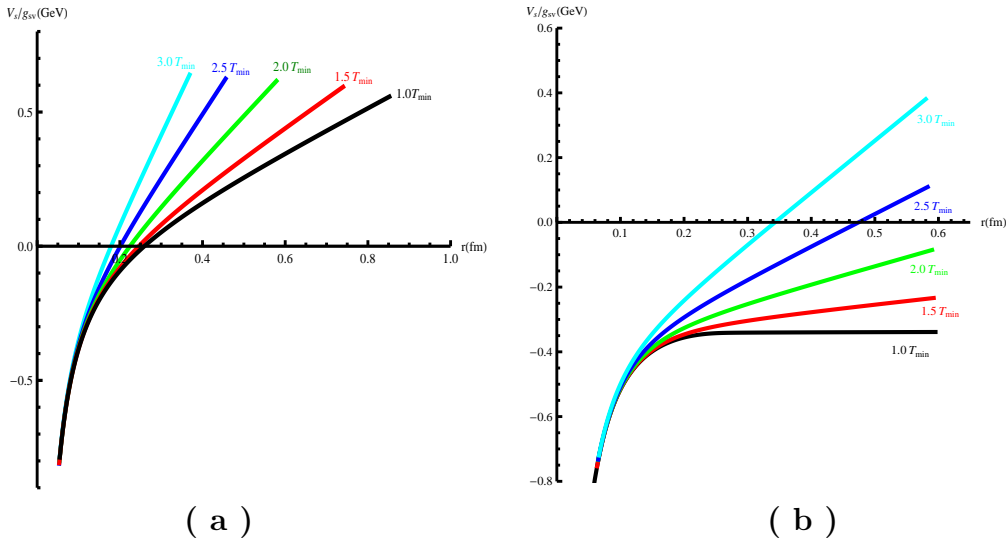


**Figure 11:** The spatial heavy quark potential  $V_s/g_{sv}$  as a function the distance between the quark anti-quark  $r$ : (a) for the case of  $c = +$  with  $k = 0.43\text{GeV}$ , (b) for the case of  $c = -$  with  $k = 0.43\text{GeV}$ .

potential is flat at lower temperature, however, when the temperature is high enough, we observe that a linear potential rises up.

Following the procedure introduced in Appendix C, we subtract the spatial string tension  $\sigma_s(T)$  and show the numerical results in Fig. 12, where the lattice data for pure  $SU(2)$  and  $SU(3)$  gauge theory are taken from [59] and [25] respectively. For the case of  $c = +$ , it is observed that the result of the spatial string tension fits very well with the lattice data in Ref.[25][59]. While for the model with negative quadratic correction, i.e.  $c = -$ , we find that the spatial string tension is not in agreement with the lattice date.

## 6. Conclusion and discussion

From the previous studies of constructing the holographic QCD models to describe hadron spectra and heavy quark potential, we have observed that a quadratic correction is related to the confinement property of QCD. There are two methods to introduce the quadratic correction to hQCD models: the first method is to add it in the warp factor of the metric, the second method is in the dilaton background. However, the connection between these two methods is lack of clarification. Moreover, the sign of the quadratic correction is still under debate.

In this work, we have established a general framework for the minimal graviton-dilaton system. By solving the Einstein equations, we can self-consistently solve the dilaton background for any a given metric structure assumed in a phenomenological holographic model. Thus, the connection between the metric structure and the

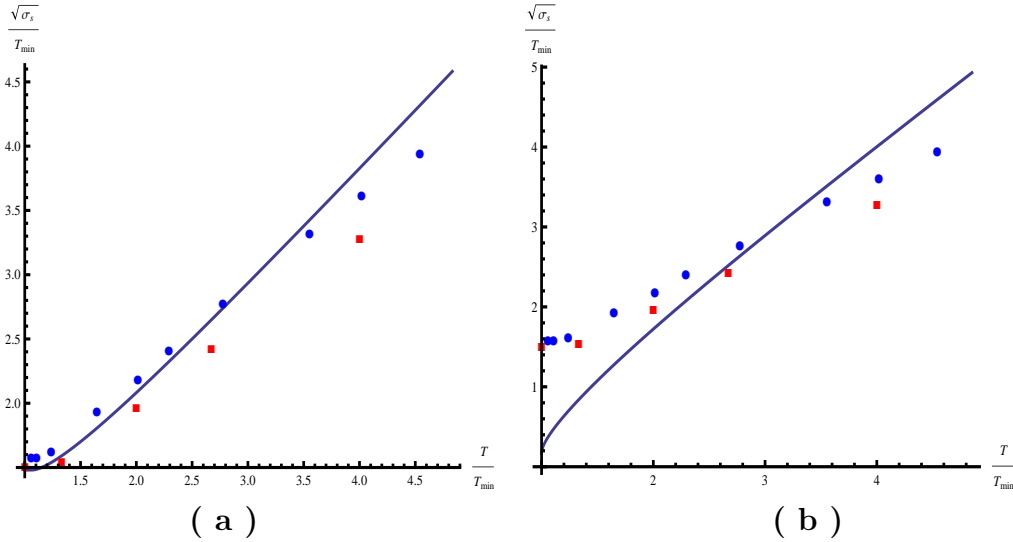


**Figure 12:** The scaled spatial string tension  $\sqrt{\sigma_s}/T_{min}$  as a function of the scaled temperature  $T/T_{min}$  for the case of  $c = +$  in (a) with  $k = 0.43\text{GeV}$  and  $g_{sv} = 0.55$  are used, and  $c = -$  in (b) with  $k = 0.43\text{GeV}$  and  $g_{sv} = 0.7$  are used, respectively. The blue dots stands for lattice data for pure  $SU(3)$  gauge theory from [25]. The red dots are lattice data as a function of  $T/T_c$  for pure  $SU(2)$  gauge theory which is from [59].

dilaton background is clearly revealed. Furthermore, we can observe: In the first method, the dilaton field should be solved out and its contribution must be taken into account; In the second method, the back-reaction of the dilaton background to the metric should be considered. In other words, both methods to introduce the quadratic correction are not self-consistent.

In this work, we extend the graviton-dilaton system to finite temperature with a dual black-hole and self-consistently study the sign of the quadratic correction in the deformed warp factor by systematically investigating the thermodynamical properties and comparing with lattice QCD on the results of the equation of state, the heavy quark potential, the spatial Wilson loop and the Polyakov loop. We find that the bulk thermodynamical properties are not sensitive to the sign of the quadratic correction, and the results of both deformed holographic QCD models with a positive and negative quadratic correction agree well with lattice QCD results for pure  $SU(3)$  gauge theory. However, the results from loop operator favor a positive quadratic correction, which agree well with lattice results. Especially, the result from the Polyakov loop excludes the model with negative quadratic correction in the warp factor of  $\text{AdS}_5$ .

We would like to make one comment that the model with a quadratic correction in the warp factor is not equivalent to the model with a quadratic correction in the dilaton background. Therefore, our result does not indicate the failure of the KKSS model, where the negative quadratic correction is introduced in the dilaton

background. This deserves further study.

It is interesting to ask the question why the bulk thermodynamical properties, such as the energy density, sound velocity, are not sensitive to the sign of the quadratic correction in the deformed warp factor, while the thermodynamical properties of loop operators favor the positive quadratic correction model. The answer to this question is offered below. The crucial point lies in that fact that the bulk thermodynamical properties are defined in the Einstein frame, and the thermal properties of loop operators are defined in the string frame. In Fig.13 (b), we can observe that for positive and negative quadratic correction, the two warp factors in the Einstein frame are almost the same. Therefore, the bulk thermodynamical properties are not sensitive to the sign of the quadratic correction. However, in Fig.13 (a), we can observe that for positive and negative quadratic correction, the two warp factors in the string frame are quite sharp. This explains why loop operators are sensitive to the sign of the quadratic correction.

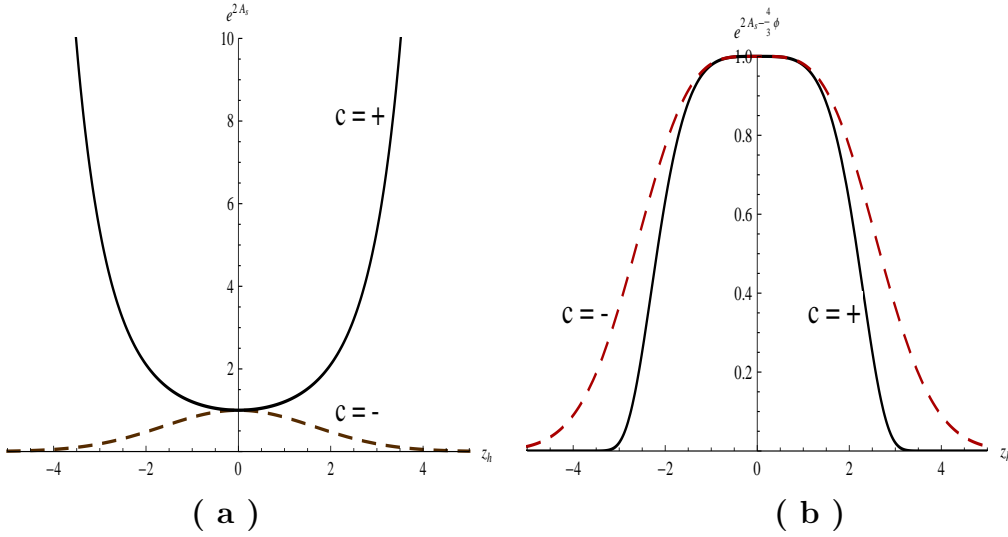


**Figure 13:** The warp factor in the string frame (a) and Einstein frame (b) for  $c = \pm$ .

### Acknowledgments:

The authors thank O.Andreev, H. Liu, D.T. Son, Y. Tian, J.B. Wu, J.F. Wu, X.N. Wu, W. Wang, and W.S. Xu and Y. Yang for valuable discussions. S.H. thanks the support from the "TOP-100" project in GUCAS. The work of M.H. is supported by CAS program "Outstanding young scientists abroad brought-in", CAS key project KJCX2-EW-N01, NSFC10735040, NSFC10875134, and K.C.Wong Education Foundation, Hong Kong.

# APPENDIX

## A. Some simple analytical black hole solutions

In this appendix, we work out two analytical gravity solutions of graviton-dilaton system by using Eq.(2.21) for given metric ansatz in Einstein frame Eq.(2.14). Here we are interested in the solutions whose UV behavior is asymptotic  $AdS_5$ . We also impose the constrains which are  $f(0) = 1$  near the  $z \sim 0$ , and requiring  $\phi(z), f(z)$  to be regular at  $z = 0, z_h$ .

To avoid misunderstanding, we should clarify that we will list two analytical gravity solutions in the Einstein frame. The metric ansatz in the Einstein takes the following form:

$$ds_E^2 = \frac{L^2 e^{2A_s - \frac{4\phi}{3}}}{z^2} \left( -f(z)dt^2 + \frac{dz^2}{f(z)} + dx^i dx^i \right) \quad (\text{A.1})$$

$$= \frac{L^2 e^{2A_E}}{z^2} \left( -f(z)dt^2 + \frac{dz^2}{f(z)} + dx^i dx^i \right). \quad (\text{A.2})$$

Where  $A_s(z)$  and  $\phi(z)$  is defined by Eq.(2.12) and Eq. (2.13) and  $A_E(z) = A_s(z) - \frac{2\phi(z)}{3}$ .

Using the general solutions in Eq.(2.21), one can easily find some exact new gravity solutions. Here, we do not repeat the procedure and details of the calculation to obtain the new gravity solutions, we just list two simple analytical gravity solutions for example.

The first solution is given as following:

$$\begin{aligned} A_E(z) &= \log \left( \frac{z}{z_0 \sinh(\frac{z}{z_0})} \right), \\ f(z) &= 1 - \frac{V_1}{3} \left( 2 - 3 \cosh\left(\frac{z}{z_0}\right) + \cosh^3\left(\frac{z}{z_0}\right) \right), \\ \phi(z) &= \frac{3z}{2z_0}. \end{aligned} \quad (\text{A.3})$$

Where  $z_0$  is integral constants and  $V_1$  is the constant from the dilaton potential

$$V_E(\phi) = -\frac{16V_1(\sinh^6(\frac{\phi}{3})) + 9(\sinh^2(\frac{2\phi}{3})) + 12}{L^2}. \quad (\text{A.4})$$

The solution above is given by the graviton-dilaton system (2.12) with nontrivial dilaton potential  $V_E$ . Where the subscript  $E$  stands for the dilaton potential in the Einstein frame. Here we should emphasize that the exact relation of the dilaton potential between the Einstein frame and string frame is given by the Eq. (2.11).



The second new gravity solution is as below:

$$A_E(z) = -\log\left(1 + \frac{z}{z_0}\right), \quad (\text{A.5})$$

$$f(z) = 1 - V_2 \left( \frac{z^7}{7z_0^7} + \frac{z^6}{2z_0^6} + \frac{3z^5}{5z_0^5} + \frac{z^4}{4z_0^4} \right), \quad (\text{A.6})$$

$$\phi(z) = 3\sqrt{2} \sinh^{-1} \left( \sqrt{\frac{z}{z_0}} \right). \quad (\text{A.7})$$

Where  $z_0$  is integral constants and  $V_2$  are the constants from the dilaton potential

$$V_E(\phi) = -\frac{3V_2 \sinh^{14} \left( \frac{\phi}{3\sqrt{2}} \right)}{35L^2} - \frac{3V_2 \sinh^{12} \left( \frac{\phi}{3\sqrt{2}} \right)}{10L^2} - \frac{3V_2 \sinh^{10} \left( \frac{\phi}{3\sqrt{2}} \right)}{10L^2} \\ - \frac{42 \sinh^4 \left( \frac{\phi}{3\sqrt{2}} \right)}{L^2} - \frac{42 \sinh^2 \left( \frac{\phi}{3\sqrt{2}} \right)}{L^2} - \frac{12}{L^2}. \quad (\text{A.8})$$

In this context, we do not discuss the application of the above two gravity solutions, such as the thermal dynamical quantities and stability of the two black hole solutions, which are left to the future work.

## B. Free energy density at UV boundary for the hQCD model with $A_s(z) = ck^2z^2$

We offer the details to derive the free-energy density at UV boundary  $z = \epsilon \rightarrow 0$  for the hQCD model with  $A_s(z) = ck^2z^2$  described in Section 3.

For black-hole case, the solutions in Section 3 expanded around UV boundary have the following expressions:

$$\phi(z) = \frac{3c}{2}k^2z^2 + \frac{3}{10}k^4z^4 + \frac{4c}{35}k^6z^6 + \frac{4}{105}k^8z^8 + o(z^9), \quad (\text{B.1})$$

$$f(z) = 1 - \frac{f_c^h}{4}k^4z^4 - \frac{3f_c^h}{40}k^8z^8 + o(z^9), \quad (\text{B.2})$$

$$A_E(z) = -\frac{1}{5}k^4z^4 - \frac{8c}{105}k^6z^6 - \frac{8}{315}k^8z^8 + o(z^9). \quad (\text{B.3})$$

For the case of thermal gas, the solutions at UV boundary take the expression as:

$$\phi_0(z) = p_2k^2z^2 + \frac{2p_2^2}{15}k^4z^4 + \frac{p_2^3(128 - 105f_c^h)}{3780}k^6z^6 \\ + \frac{p_2^4(64 - 63f_c^h)}{8505}k^8z^8 + o(z^9), \quad (\text{B.4})$$

$$f_0(z) = 1, \quad (\text{B.5})$$

$$A_{E0}(z) = -\frac{4p_2^2}{45}k^4z^4 - \frac{64p_2^3}{2835}k^6z^6 + \frac{p_2^4(-128 + 105f_c^h)}{25515}k^8z^8 + o(z^9). \quad (\text{B.6})$$

To compare the free-energy density of the black-hole case and the thermal gas case, one has to impose the following conditions [49]:

$$\phi_0(z) |_{\epsilon=} = \phi(z) |_{\epsilon}, \quad (\text{B.7})$$

$$\tilde{\beta}b_0(z) |_{\epsilon=} = \beta b(z) |_{\epsilon}, \quad (\text{B.8})$$

$$\tilde{V}_3 b_0^3(z) |_{\epsilon=} = V_3 b^3(z) |_{\epsilon}. \quad (\text{B.9})$$

Comparing Eq.(B.3) with Eq.(B.6), we can get the relationship between  $p_2$  and  $k$ ,

$$p_2 = \frac{3}{2}c \left( 1 + \frac{1}{16}k^4 f_c^h \epsilon^4 + \frac{k^8 (-128f_c^h + 105(f_c^h)^2) \epsilon^8}{8960} + o(\epsilon^9) \right). \quad (\text{B.10})$$

Then we get the free energy densities for the black-hole and thermal gas at UV boundary as follows:

$$\begin{aligned} \mathcal{F}_{BH}^\epsilon &= 2M^3 \left( 3b(\epsilon)^2 f(\epsilon) b'(\epsilon) + \frac{1}{2}b(\epsilon)^3 f'(\epsilon) \right) \\ &= -\frac{6(L^3 M^3)}{\epsilon^4} - \left( \frac{6}{5}k^4 L^3 M^3 - \frac{1}{2}k^4 L^3 M^3 f_c^h \right) + o(\epsilon^2) \end{aligned} \quad (\text{B.11})$$

$$\begin{aligned} \mathcal{F}_{TG}^\epsilon &= \frac{2M^3 \left( b(\epsilon)^4 \sqrt{f(\epsilon)} \right) \left( 3b_0(\epsilon)^2 f_0(\epsilon) b_0'(\epsilon) + \frac{1}{2}b_0(\epsilon)^3 f_0'(\epsilon) \right)}{b_0(\epsilon)^4 \sqrt{f_0(\epsilon)}} \\ &= -\frac{6L^3 M^3}{\epsilon^4} - \left( \frac{6}{5}k^4 L^3 M^3 - \frac{3}{4}k^4 L^3 M^3 f_c^h \right) + o(\epsilon^2). \end{aligned} \quad (\text{B.12})$$

From the above result, one can derive the free energy density difference as follows:

$$\Delta\mathcal{F} = -\frac{1}{4}k^4 M^3 L^3 f_c^h - 2M^3 b_0^2(z_{IR}) b_0'(z_{IR}). \quad (\text{B.13})$$

From Eqs.(3.3),(4.3) and (4.19), one can express the temperature dependent coefficient  $f_c^h$  with the entropy density and temperature as

$$f_c^h = \frac{16\pi G_5}{k^4 L^3} T s = \frac{T s}{k^4 M^3 L^3}. \quad (\text{B.14})$$

As a result, one gets

$$\Delta\mathcal{F} = -\frac{1}{4}T s - 2M^3 b_0^2(z_{IR}) b_0'(z_{IR}). \quad (\text{B.15})$$

### C. To extract the spatial string tension

In this appendix, we show how to extract the spatial string tension. A first-principle method for determining the spatial string tension in hot QCD matter is to measure

the rectangular spatial Wilson loops as we show in Sec.5.3. The spatial potential  $V_s(r)$  is defined by:

$$V_s(r) = - \lim_{Y \rightarrow \infty} \frac{1}{r} \log W(r, Y). \quad (\text{C.1})$$

The spatial string tension can be obtained:

$$\sigma_s(T) = \lim_{r \rightarrow \infty} \frac{V_s(r)}{r}. \quad (\text{C.2})$$

To extract the spatial string tension, one can use the following relation:

$$V_s = S_{xy} \sim \sigma_s r \quad r \gg 1. \quad (\text{C.3})$$

Under the general background

$$ds^2 = \frac{L^2 e^{2A_s}}{z^2} \left( f(z) dt^2 + \frac{dz^2}{f(z)} + dx^i dx^i \right), \quad (\text{C.4})$$

the separation of the two static quarks has the form of:

$$r(z_0) = z_0 \int_0^1 \frac{2\nu^2 e^{2A_s(z_0) - 2A_s(\nu z_0)}}{\sqrt{f(\nu z_0) (1 - \nu^4 e^{4A_s(z_0) - 4A_s(\nu z_0)})}} d\nu. \quad (\text{C.5})$$

The free energy of the spatial Wilson loop is given by:

$$S_{xy}(z_0) = \frac{g_{sv}}{\pi z_0} \int_0^1 \frac{1}{\nu^2} \frac{e^{2A_s(\nu z_0)}}{\sqrt{f(\nu z_0) (1 - \nu^4 e^{4A_s(z_0) - 4A_s(\nu z_0)})}} d\nu. \quad (\text{C.6})$$

We assume that the function  $A_s(z_0)$  is a regular function here. One should focus on the denominator of the Eq.(C.5) and Eq.(C.6) which make main contribution to the integral when  $\nu \sim 1$ . If one just focus on the dominant part, one can expand the denominators at  $\nu = 1$  respectively. After the expansion up to the order  $O((\nu - 1)^2)$  and integral out the formula, one can find the coefficient:

$$\begin{aligned} & (1 - \nu) (-4z_0 f(z_0) A'_s(z_0) + 4f(z_0)) \\ & + (1 - \nu)^2 \left( 4z_0^2 f'(z_0) A'_s(z_0) - 8z_0^2 f(z_0) A'_s(z_0)^2 + 24z_0 f(z_0) A'_s(z_0) \right. \\ & \left. + 2z_0^2 f(z_0) A''_s(z_0) - 4z_0 f'(z_0) - 14f(z_0) \right) \end{aligned} \quad (\text{C.7})$$

In term of the following useful integral formula:

$$\int_0^1 \frac{1}{\sqrt{a(1-\nu) + b(1-\nu)^2}} = \frac{2 \text{ArcTanh} \left( \sqrt{\frac{b}{a+b}} \right)}{\sqrt{b}}, \quad a > 0 \quad \text{and} \quad b > 0, \quad (\text{C.8})$$

one can notice that the integral will be divergent when  $a = 0$ .  $r(z_0)$  can be obtained and has the form of

$$r(z_0) = \frac{4z_0 \tanh^{-1} \left( \frac{\sqrt{b_L}}{\sqrt{a_L + b_L}} \right)}{\sqrt{b_L}} + O(1) \quad (\text{C.9})$$

with  $a_L$  and  $b_L$  the coefficients appeared in Eq.(C.8) respectively.

Following the same strategy, we can get the spatial potential

$$V_s(z_0) = \frac{2e^{2A_s(z_0)} \tanh^{-1} \left( \frac{\sqrt{b_V}}{\sqrt{a_V + b_V}} \right)}{\pi z_0 \sqrt{b_V}} + O(1). \quad (\text{C.10})$$

Where  $a_V$  and  $b_V$  are the coefficients mentioned in Eq.(C.8) respectively. Comparing Eq.(C.9) and Eq.(C.10), one can easily get the spatial string tension. Up to the order  $O(1 - \nu)^2$ , the coefficients listed in Eq.C.7 have the following exact relations such as  $a_L = a_V$  and  $b_L = b_V$  in Eq.(C.9) and Eq.(C.10). The spatial string tension has the form of

$$\sigma_s/g_{sv} = \frac{e^{2A_s(z_h)}}{2\pi z_h^2}, \quad (\text{C.11})$$

Here, One can find that the spatial string tension  $\sigma_s$  depends on the warp factor  $A_s(z)$ . In pure  $AdS_5$  case,

$$\sigma_s/g_{sv} = \frac{1}{2\pi z_h^2}. \quad (\text{C.12})$$

## References

- [1] J. M. Maldacena, “The large N limit of superconformal field theories and supergravity,” *Adv. Theor. Math. Phys.* **2**, 231 (1998) [*Int. J. Theor. Phys.* **38**, 1113 (1999)]; S. S. Gubser, I. R. Klebanov and A. M. Polyakov, “Gauge theory correlators from non-critical string theory,” *Phys. Lett. B* **428**, 105 (1998); E. Witten, “The large N limit of superconformal field theories and supergravity,” *Adv.Theor.Math.Phys.* **2** (1998) 253-291.
- [2] P. Kovtun, D. T. Son and A. O. Starinets, “Viscosity in strongly interacting quantum field theories from black hole physics,” *Phys. Rev. Lett.* **94**, 111601 (2005) [[arXiv:hep-th/0405231](#)].
- [3] A. Buchel and J. T. Liu, “Universality of the shear viscosity in supergravity,” *Phys. Rev. Lett.* **93**, 090602 (2004); K. Maeda, M. Natsuume and T. Okamura, “Viscosity of gauge theory plasma with a chemical potential from AdS/CFT,” *Phys. Rev. D* **73**, 066013 (2006); M. Brigante, H. Liu, R. C. Myers, S. Shenker and S. Yaida, “The Viscosity Bound and Causality Violation,” *Phys. Rev. Lett.* **100**, 191601 (2008); R. G. Cai, Z. Y. Nie, N. Ohta and Y. W. Sun, “Shear Viscosity from Gauss-Bonnet Gravity with a Dilaton Coupling,” *Phys. Rev. D* **79**, 066004 (2009);
- [4] Y. Kim, Y. Seo and S. J. Sin, “Nuclear matter to strange matter transition in holographic QCD,” [arXiv:0911.3685](#) [hep-th]. K. Jo, B. H. Lee, C. Park and S. J. Sin, “Holographic QCD in medium: a bottom up approach,” [arXiv:0909.3914](#) [hep-ph]. K. Y. Kim, S. J. Sin and I. Zahed, “Dense and Hot Holographic QCD: Finite Baryonic E Field,” *JHEP* **0807**, 096 (2008).

- [5] S. S. Gubser and A. Nellore, “Mimicking the QCD equation of state with a dual black hole,” *Phys. Rev. D* **78**, 086007 (2008); S. S. Gubser, A. Nellore, S. S. Pufu and F. D. Rocha, “Thermodynamics and bulk viscosity of approximate black hole duals to finite temperature quantum chromodynamics,” *Phys. Rev. Lett.* **101**, 131601 (2008); S. S. Gubser, S. S. Pufu and F. D. Rocha, “Bulk viscosity of strongly coupled plasmas with holographic duals,” *JHEP* **0808**, 085 (2008).
- [6] U. Gursoy, E. Kiritsis, L. Mazzanti and F. Nitti, *JHEP* **0905**, 033 (2009);
- [7] U. Gursoy, E. Kiritsis, L. Mazzanti and F. Nitti, “Deconfinement and Gluon Plasma Dynamics in Improved Holographic QCD,” *Phys. Rev. Lett.* **101**, 181601 (2008); U. Gursoy, E. Kiritsis, G. Michalogiorgakis and F. Nitti, “Thermal Transport and Drag Force in Improved Holographic QCD,” *JHEP* **0912**, 056 (2009).
- [8] E. Megias, H. J. Pirner and K. Veschgini, “QCD-Thermodynamics using 5-dim Gravity,” *Phys. Rev. D* **83**, 056003 (2011); K. Veschgini, E. Megias and H. J. Pirner, “Trouble Finding the Optimal AdS/QCD,” arXiv:1009.4639 [hep-th].
- [9] O. Andreev, “Some Thermodynamic Aspects of Pure Glue, Fuzzy Bags and Gauge/String Duality,” *Phys. Rev. D* **76**, 087702 (2007) [arXiv:0706.3120 [hep-ph]].
- [10] O. Andreev and V. I. Zakharov, “The Spatial String Tension, Thermal Phase Transition, and AdS/QCD,” *Phys. Lett. B* **645**, 437 (2007) [arXiv:hep-ph/0607026]; O. Andreev, “The Spatial String Tension in the Deconfined Phase of SU(N) Gauge Theory and Gauge/String Duality,” *Phys. Lett. B* **659**, 416 (2008) [arXiv:0709.4395 [hep-ph]].
- [11] O. Andreev and V. I. Zakharov, “On Heavy-Quark Free Energies, Entropies, Polyakov Loop, and AdS/QCD,” *JHEP* **0704**, 100 (2007) [arXiv:hep-ph/0611304];
- [12] O. Andreev, “Renormalized Polyakov Loop in the Deconfined Phase of SU(N) Gauge Theory and Gauge/String Duality,” *Phys. Rev. Lett.* **102**, 212001 (2009) [arXiv:0903.4375 [hep-ph]].
- [13] J. Noronha, “Connecting Polyakov Loops to the Thermodynamics of  $SU(N_c)$  Gauge Theories Using the Gauge-String Duality,” *Phys. Rev. D* **81**, 045011 (2010) [arXiv:0910.1261 [hep-th]].
- [14] K. Kajantie, T. Tahkokallio and J. T. Yee, “Thermodynamics of AdS/QCD,” *JHEP* **0701**, 019 (2007) [arXiv:hep-ph/0609254]; J. Alanen, K. Kajantie and V. Suur-Uski, “A gauge/gravity duality model for gauge theory thermodynamics,” *Phys. Rev. D* **80**, 126008 (2009) [arXiv:0911.2114 [hep-ph]]; J. Alanen, K. Kajantie and V. Suur-Uski, “Spatial string tension of finite temperature QCD matter in gauge/gravity duality,” *Phys. Rev. D* **80**, 075017 (2009) [arXiv:0905.2032 [hep-ph]].
- [15] D. Teaney, J. Lauret and E. V. Shuryak, “Flow at the SPS and RHIC as a quark gluon plasma signature,” *Phys. Rev. Lett.* **86**, 4783 (2001) [arXiv:nucl-th/0011058];

- P. Huovinen, P. F. Kolb, U. W. Heinz, P. V. Ruuskanen and S. A. Voloshin, “Radial and elliptic flow at RHIC: Further predictions,” *Phys. Lett. B* **503**, 58 (2001) [arXiv:hep-ph/0101136]; T. Hirano, U. W. Heinz, D. Kharzeev, R. Lacey and Y. Nara, “Hadronic dissipative effects on elliptic flow in ultrarelativistic heavy-ion collisions,” *Phys. Lett. B* **636**, 299 (2006) [arXiv:nucl-th/0511046]; P. Romatschke and U. Romatschke, “Viscosity Information from Relativistic Nuclear Collisions: How Perfect is the Fluid Observed at RHIC?,” *Phys. Rev. Lett.* **99**, 172301 (2007) [arXiv:0706.1522 [nucl-th]]; H. Song and U. W. Heinz, “Suppression of elliptic flow in a minimally viscous quark-gluon plasma,” *Phys. Lett. B* **658**, 279 (2008) [arXiv:0709.0742 [nucl-th]]; H. Song and U. W. Heinz, “Causal viscous hydrodynamics in 2+1 dimensions for relativistic heavy-ion collisions,” *Phys. Rev. C* **77**, 064901 (2008) [arXiv:0712.3715 [nucl-th]].
- [16] D. Teaney, *Phys. Rev. C* **68**, 034913 (2003).
- [17] I. Arsene *et al.* [BRAHMS Collaboration], *Nucl. Phys. A* **757**, 1 (2005), K. Adcox *et al.* [PHENIX Collaboration], *Nucl. Phys. A* **757**, 184 (2005), B. B. Back *et al.*, *Nucl. Phys. A* **757**, 28 (2005), J. Adams *et al.* [STAR Collaboration], *Nucl. Phys. A* **757**, 102 (2005).
- [18] M. Gyulassy and L. McLerran, *Nucl. Phys. A* **750**, 30 (2005).
- [19] D. Kharzeev and K. Tuchin, *JHEP* **0809**, 093 (2008).
- [20] F. Karsch, D. Kharzeev and K. Tuchin, “Universal properties of bulk viscosity near the QCD phase transition,” *Phys. Lett. B* **663**, 217 (2008) [arXiv:0711.0914 [hep-ph]].
- [21] H. B. Meyer, “A calculation of the bulk viscosity in SU(3) gluodynamics,” *Phys. Rev. Lett.* **100**, 162001 (2008) [arXiv:0710.3717 [hep-lat]].
- [22] K. Paech and S. Pratt, “Origins of bulk viscosity at RHIC,” *Phys. Rev. C* **74**, 014901 (2006) [arXiv:nucl-th/0604008].
- [23] B. C. Li and M. Huang, “Non-conformality and non-perfectness of fluid near phase transition,” *Phys. Rev. D* **78**, 117503 (2008) arXiv:0807.0292 [hep-ph]; B. C. Li and M. Huang, “Thermodynamic properties and bulk viscosity near phase transition in the Z(2) and O(4) models,” *Phys. Rev. D* **80**, 034023 (2009) [arXiv:0903.3650 [hep-ph]]; H. Mao, J. Jin and M. Huang, “Phase diagram and thermodynamics of the Polyakov linear sigma model with three quark flavors,” *J. Phys. G* **37**, 035001 (2010) [arXiv:0906.1324 [hep-ph]].
- [24] J. W. Chen and J. Wang, “Bulk Viscosity of a Gas of Massless Pions,” *Phys. Rev. C* **79**, 044913 (2009) arXiv:0711.4824 [hep-ph].
- [25] G. Boyd, J. Engels, F. Karsch, E. Laermann, C. Legeland, M. Lutgemeier and B. Petersson, “Thermodynamics of SU(3) Lattice Gauge Theory,” *Nucl. Phys. B* **469**, 419 (1996) [arXiv:hep-lat/9602007].

- [26] M. Cheng *et al.*, “The QCD Equation of State with almost Physical Quark Masses,” *Phys. Rev. D* **77**, 014511 (2008) [arXiv:0710.0354 [hep-lat]].
- [27] J. Erlich, E. Katz, D. T. Son and M. A. Stephanov, “QCD and a holographic model of hadrons,” *Phys. Rev. Lett.* **95**, 261602 (2005).
- [28] G. F. de Teramond and S. J. Brodsky, “The hadronic spectrum of a holographic dual of QCD,” *Phys. Rev. Lett.* **94**, 201601 (2005).
- [29] L. Da Rold and A. Pomarol, “Chiral symmetry breaking from five dimensional spaces,” *Nucl. Phys. B* **721**, 79 (2005).
- [30] J. Babington, J. Erdmenger, N. J. Evans, Z. Guralnik and I. Kirsch, “Chiral symmetry breaking and pions in non-supersymmetric gauge/gravity *Phys. Rev. D* **69**, 066007 (2004) [arXiv:hep-th/0306018].
- [31] M. Kruczenski, D. Mateos, R. C. Myers and D. J. Winters, *JHEP* 0405 (2004) 041.
- [32] T. Sakai and S. Sugimoto, “Low energy hadron physics in holographic QCD,” *Prog. Theor. Phys.* **113**, 843 (2005); [arXiv:hep-th/0412141]. T. Sakai and S. Sugimoto, “More on a holographic dual of QCD,” *Prog. Theor. Phys.* **114**, 1083 (2006). [arXiv:hep-th/0507073].
- [33] S. He, M. Huang, Q. S. Yan and Y. Yang, “Confront Holographic QCD with Regge Trajectories,” *Eur.Phys.J.C.*(2010)66:187. arXiv:0710.0988 [hep-ph].
- [34] A. Karch, E. Katz, D. T. Son and M. A. Stephanov, “Linear Confinement and AdS/QCD,” *Phys. Rev. D* **74**, 015005 (2006) [arXiv:hep-ph/0602229].
- [35] O. Andreev and V. I. Zakharov, “Heavy-quark potentials and AdS/QCD,” *Phys. Rev. D* **74**, 025023 (2006) [arXiv:hep-ph/0604204].
- [36] F. Zuo, “Improved Soft-Wall model with a negative dilaton,” *Phys. Rev. D* **82**, 086011 (2010). arXiv:0909.4240 [hep-ph].
- [37] G. F. de Teramond and S. J. Brodsky, “Light-Front Holography and Gauge/Gravity Duality: The Light Meson and Baryon Spectra,” arXiv:0909.3900 [hep-ph].
- [38] J. P. Shock, F. Wu, Y. L. Wu and Z. F. Xie, “AdS/QCD phenomenological models from a back-reacted geometry,” *JHEP* **0703**, 064 (2007).
- [39] K. Ghoroku, M. Tachibana and N. Uekusa, “Dilaton coupled brane-world and field trapping,” *Phys. Rev. D* **68**, 125002 (2003); [arXiv:hep-th/0304051]. K. Ghoroku, N. Maru, M. Tachibana and M. Yahiro, “Holographic model for hadrons in deformed AdS(5) background,” *Phys. Lett. B* **633**, 602 (2006). [arXiv:hep-ph/0510334].
- [40] C. Csaki and M. Reece, “Toward a systematic holographic QCD: A braneless approach,” *JHEP* **0705**, 062 (2007) [arXiv:hep-ph/0608266].

- [41] U. Gursoy and E. Kiritsis, “Exploring improved holographic theories for QCD: Part I,” *JHEP* **0802**, 032 (2008); [arXiv:0707.1324 [hep-th]]. U. Gursoy, E. Kiritsis and F. Nitti, “Exploring improved holographic theories for QCD: Part II,” *JHEP* **0802**, 019 (2008). [arXiv:0707.1349 [hep-th]].
- [42] D. f. Zeng, “Heavy quark potentials in some renormalization group revised AdS/QCD models,” *Phys. Rev. D* **78**, 126006 (2008) [arXiv:0805.2733 [hep-th]].
- [43] H. J. Pirner and B. Galow, “Strong Equivalence of the AdS-Metric and the QCD Running Coupling,” *Phys. Lett. B* **679**, 51 (2009) [arXiv:0903.2701 [hep-ph]].
- [44] S. He, M. Huang and Q. S. Yan, “Logarithmic correction in the deformed AdS<sub>5</sub> model to produce the heavy quark potential and QCD beta function,” arXiv:1004.1880 [hep-ph].
- [45] A. Karch, E. Katz, D. T. Son and M. A. Stephanov, arXiv:1012.4813 [hep-ph].
- [46] J. Polchinski, *String Theory*, vol.2 Cambridge University Press,1998; K. Becker, M. Becker, J. H. Schwarz, *String Theory and M-theory*, Cambridge University Press,2006.
- [47] F. V. Gubarev, L. Stodolsky and V. I. Zakharov, “On the significance of the quantity  $A^{**2}$ ,” *Phys. Rev. Lett.* **86**, 2220 (2001) [arXiv:hep-ph/0010057]; F. V. Gubarev and V. I. Zakharov, “On the emerging phenomenology of  $\langle(A(a)(\mu))^{**2}(\min)\rangle$ ,” *Phys. Lett. B* **501**, 28 (2001) [arXiv:hep-ph/0010096].
- [48] C. P. Herzog, *Phys. Rev. Lett.* **98**, 091601 (2007). [hep-th/0608151].
- [49] S.W. Hawking,G.T. Horowitz, “The Gravitational Hamiltonian, action, entropy and surface terms” *Class. Quant. Grav.* **13**, 1487.
- [50] S. W. Hawking and D. N. Page, “Thermodynamics Of Black Holes In Anti-De Sitter Space,” *Commun. Math. Phys.* **87**, 577 (1983).
- [51] J. D. Bekenstein, *Phys. Rev. D* **7**, 2333 (1973); S. W. Hawking, *Commun. Math. Phys.* **43**, 199 (1975) [Erratum-ibid. **46**, 206 (1976)].
- [52] L.D. Landau, E.M. Lifshitz, et al. *Statistical Physics: Volume 5 (Course of Theoretical Physics)*, 3rd edition, Butterworth-Heinemann, Oxford, Boston, Johannesburg, Melbourne, New Delhi, Singapore, 1980.
- [53] R. V. Gavai, S. Gupta and S. Mukherjee, “The Speed of sound and specific heat in the QCD plasma: Hydrodynamics, fluctuations and conformal symmetry,” *Phys. Rev. D* **71**, 074013 (2005) [arXiv:hep-lat/0412036].
- [54] A. M. Polyakov, “Thermal Properties Of Gauge Fields And Quark Liberation,” *Phys. Lett. B* **72**, 477 (1978).



- [55] Y. Nambu and G. Jona-Lasinio, “Dynamical model of elementary particles based on an analogy with superconductivity. I,” *Phys. Rev.* **122**, 345 (1961); Y. Nambu and G. Jona-Lasinio, “Dynamical model of elementary particles based on an analogy with superconductivity. II,” *Phys. Rev.* **124**, 246 (1961); U. Vogl and W. Weise, “The Nambu and Jona Lasinio model: Its implications for hadrons and nuclei,” *Prog. Part. Nucl. Phys.* **27**, 195 (1991); S.P. Klevansky, “The Nambu-Jona-Lasinio model of quantum chromodynamics,” *Rev. Mod. Phys.* **64**, 649 (1992); T. Hatsuda and T. Kunihiro, “QCD phenomenology based on a chiral effective Lagrangian,” *Phys. Rept.* **247**, 221 (1994); R. Alkofer, H. Reinhardt and H. Weigel, *Phys. Rept.* **265**, 139 (1996).
- [56] M. Gell-Mann and M. Levy, “The Axial Vector Current In Beta Decay,” *Nuovo Cim.* **16**, 705 (1960). J. T. Lenaghan, D. H. Rischke and J. Schaffner-Bielich, “Chiral symmetry restoration at nonzero temperature in the  $SU(3)_r \times SU(3)_l$  linear sigma model,” *Phys. Rev. D* **62**, 085008 (2000) [arXiv:nucl-th/0004006].
- [57] O. Kaczmarek, F. Karsch, F. Zantow and P. Petreczky, “Static quark anti-quark free energy and the running coupling at finite temperature,” *Phys. Rev. D* **70**, 074505 (2004) [Erratum-ibid. *D* **72**, 059903 (2005)] [arXiv:hep-lat/0406036].
- [58] S. Gupta, K. Huebner and O. Kaczmarek, “Renormalized Polyakov loops in many representations,” *Phys. Rev. D* **77**, 034503 (2008) [arXiv:0711.2251 [hep-lat]].
- [59] G. S. Bali, J. Fingberg, U. M. Heller, F. Karsch and K. Schilling, “The Spatial string tension in the deconfined phase of the (3+1)-dimensional  $SU(2)$  gauge theory,” *Phys. Rev. Lett.* **71**, 3059 (1993) [arXiv:hep-lat/9306024].
- [60] J. M. Maldacena, “Wilson loops in large N field theories,” *Phys. Rev. Lett.* **80**, 4859 (1998) [arXiv:hep-th/9803002].
- [61] S. J. Rey, S. Theisen and J. T. Yee, “Wilson-Polyakov loop at finite temperature in large N gauge theory and anti-de Sitter supergravity,” *Nucl. Phys. B* **527**, 171 (1998) [arXiv:hep-th/9803135].
- [62] J. L. Albacete, Y. V. Kovchegov and A. Taliotis, “Heavy Quark Potential at Finite Temperature in AdS/CFT Revisited,” *Phys. Rev. D* **78**, 115007 (2008) [arXiv:0807.4747 [hep-th]].
- [63] E. Witten, “Anti-de Sitter space, thermal phase transition, and confinement in gauge theories,” *Adv. Theor. Math. Phys.* **2**, 505 (1998) [arXiv:hep-th/9803131].
- [64] A. M. Polyakov, “String theory and quark confinement,” *Nucl. Phys. Proc. Suppl.* **68**, 1 (1998) [arXiv:hep-th/9711002].